UNITED NATIONS EDUCATIONAL, SCIENTIFIC AND CULTURAL ORGANIZATION
INTERNATIONAL ATOMIC ENERGY AGENCY
INTERNATIONAL CENTRE FOR THEORETICAL PHYSICS
I.C.T.P., P.O. BOX 586, 34100 TRIESTE, ITALY, CABLE: CENTRATOM TRIESTE

H4.SMR/916 - 28

SEVENTH COLLEGE ON BIOPHYSICS:
Structure and Function of Biopolymers: Experimental and Theoretical Techniques.
4 - 29 March 1996

Electron Transfer in Proteins

David BERATAN
Department of Chemistry
University of Pittsburgh
Pittsburgh, Pennsylvania
U.S.A.

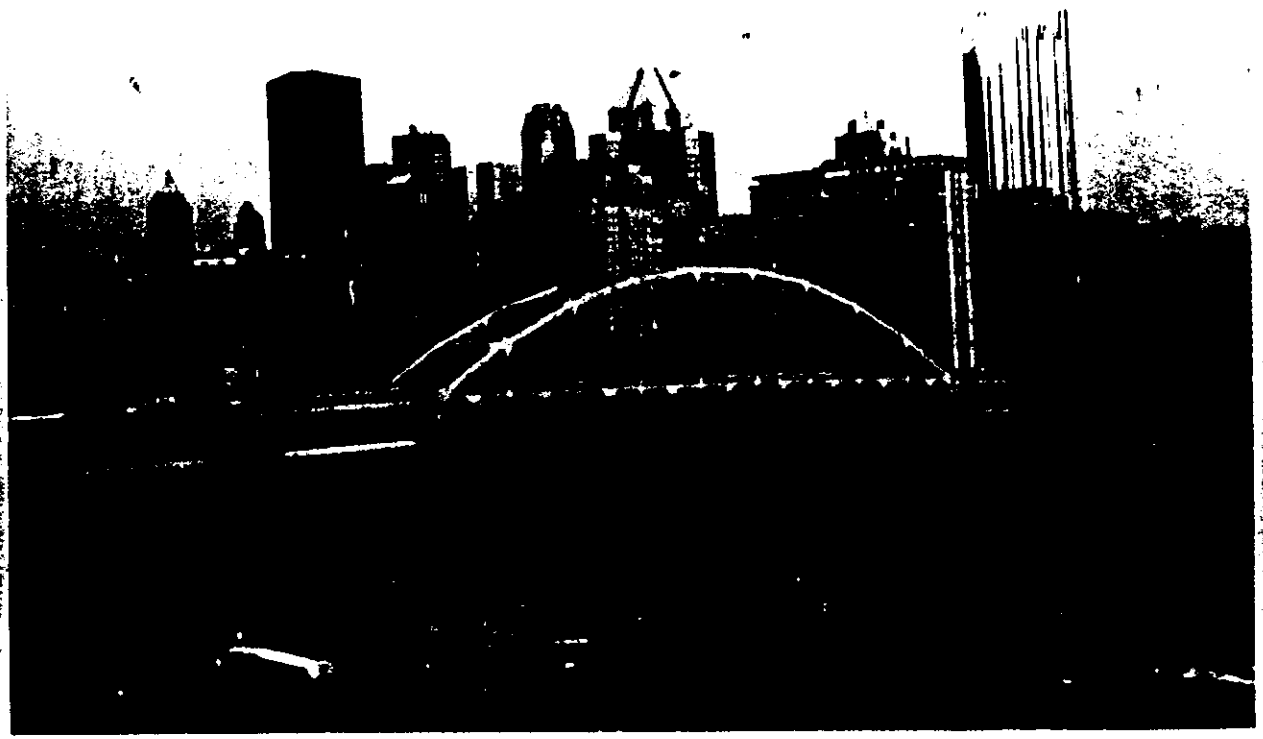

David Beratan
Dept. of Chemistry
University of Pittsburgh

Electron Transfer in Biology

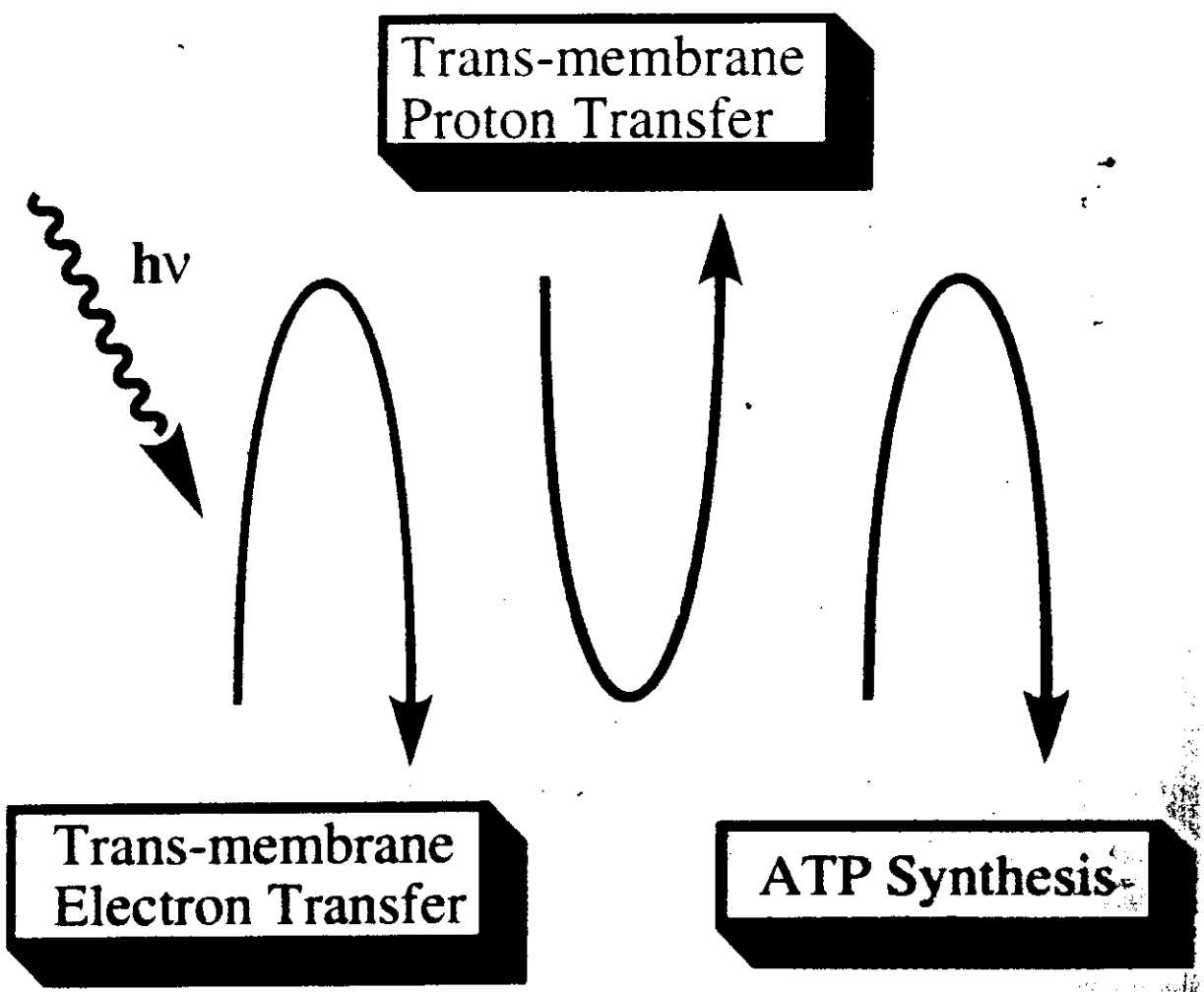

Numerous chemical rxns. & optical processes shift electron distributions without breaking bonds.

Some Examples

(1) Photosynthesis

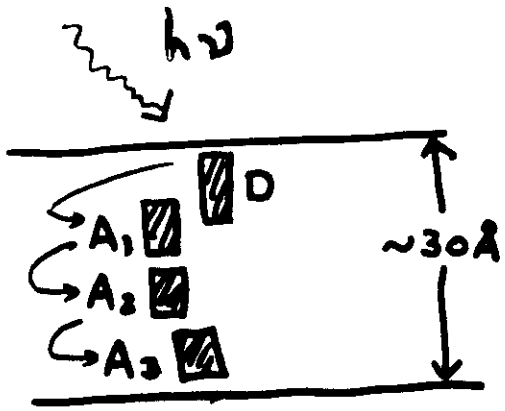

$DA_1A_2A_3$
$\downarrow h\nu$
$D^*A_1A_2A_3$ (1)
$\downarrow$ ET
$D^+A_1^-A_2A_3$ (2)
$\downarrow$ ET
$D^+A_1A_2^-A_3$ (3)
$\downarrow$ ET
$D^+A_1A_2A_3^-$ (4)

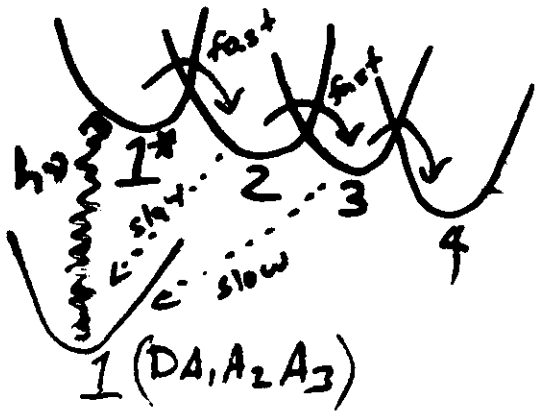

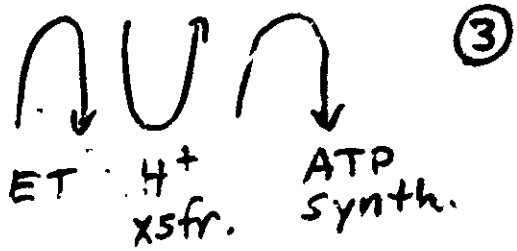

Organic
(2) Dye Chemistry

HOMO
SOMEWHAT
LOCALIZED
HERE

LUMO
SOMEWHAT
LOCALIZED
HERE

Subtle changes to D/B/A or solvent change color.

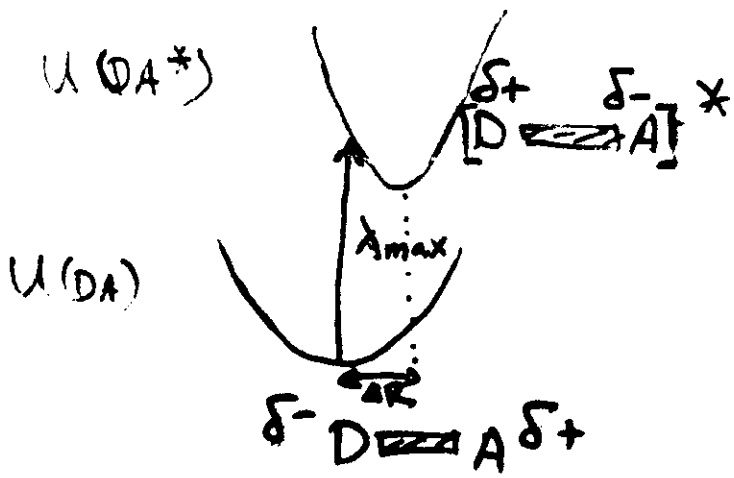

[here E.T. is induced directly by the light field.]

What defines "R"?

- nuclei in molecule
- Solvent
- counter-ion's
- ⋮

(3) Corrosion

$$M^{\circ} + \text{oxidant} \longrightarrow M^{+n}$$

(4) Self-exchange rxns.

$$Fe_A^{+2} + Fe_B^{+3} \longrightarrow Fe_A^{+3} + Fe_B^{+2}$$

These exps. motivated modern ET theory.

"Cross-relations" connect self-exchange rates with cross rates:

e.g. knowing A^{+2}/A^{+3}, B^{+2}/B^{+3} } self-ex. k's

can calc. $A^{+2} + B^{+3} \xrightarrow{k_{AB}} A^{+3} + B^{+2}$

k_{AB}

(5) Redox processes @ electrodes

(6) Solid-state ET

e.g. between defect sites in solids

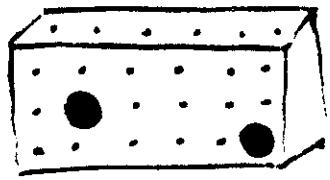

Direct photoexcitation to ET states in Metal complexes

MLCT: metal → ligand CT

LMCT: ligand → metal CT

e.g. $Ru^{+2}(bpy)_3 \xrightarrow{h\nu} Ru^{+3}(bpy)_3^{\bullet -}$

bpy = 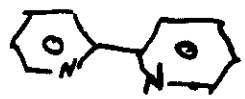

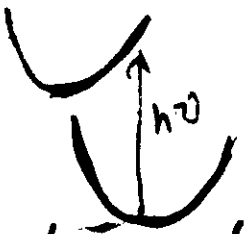

nondegenerate D/A

IVCT: metal → metal CT

M^{+n} —— M^{+n+1}

degenerate D/A

Intervalence charge transfer

Our goal:

Structure - Function relationships for Macromolecule bridged electron transfer reactions

$D^-A \rightarrow DA^-$ (1)

Lecture 1: Overview of ET Theory

Lecture 2: Protein Mediated Coupling:
(1) Pathway Methods

Lecture 3: (2) Multi-path Analysis

Rate Formulation (weakly coupled D&A):

k_{ET} ~ P (electron on D tunneling to A and being trapped)

$\sim e^{-G^{\ddagger}/RT}$

Franck-Condon Factor ~ P (coincidence of D and A energy levels)

D, A, and barrier dependent x P (Electron Tunneling from D to A)

$\sim e^{-\alpha R_{DA}}$

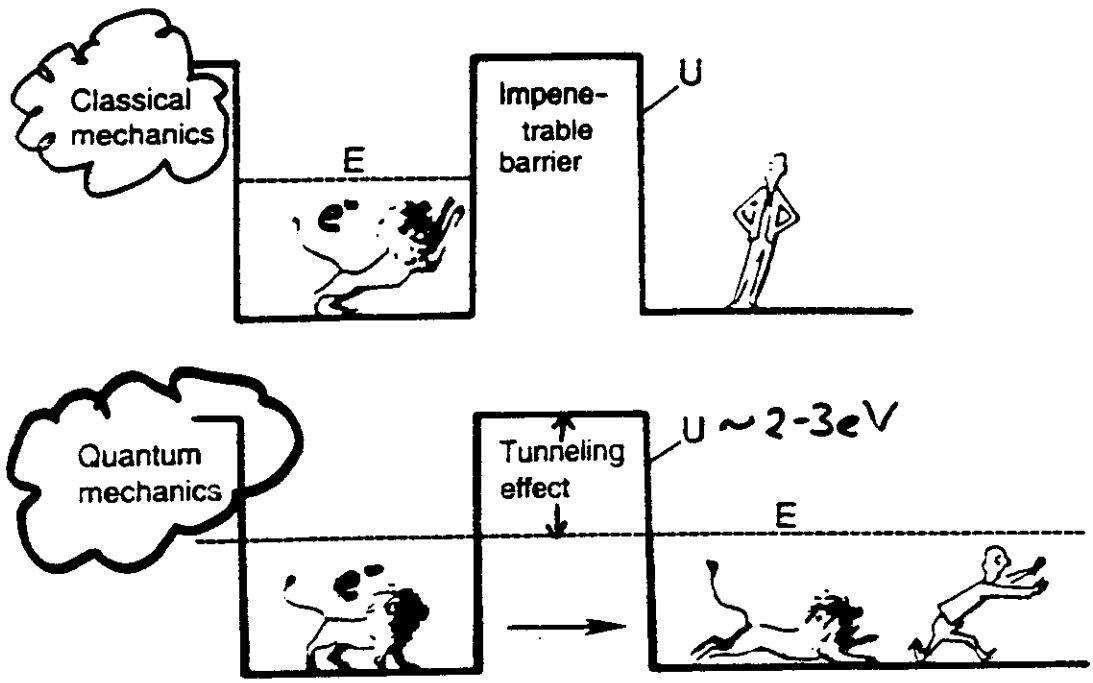

Fig. 1.3. The difference between classical theory and quantum theory

Unifying ideas/assumptions:

(1) One (usually!) e^- xfr'd per step.

many e^- processes important but not as well understood.

(2) Well defined change in charge density (D → A, electron to A, etc.)

(3) Nuclei coupled to ET move, but bonds do not break (outer sphere ET).

Core Physical Concepts

- e^-/nuc$^+$ have opposite charges, so adding/removing e^- shifts equilibrium bond lengths.
- This shift of nuclei coupled to e^- motion creates (1) nuclear activation barrier ($E_a^\ddagger$) for e^- xprt. (2) this eplg. adds structure to abs./emiss spectra, photoelectron spectra, etc.
- insufficient energy for classical transport → electron tunneling

A Few Energy Dependences

Potential Energy Wells.

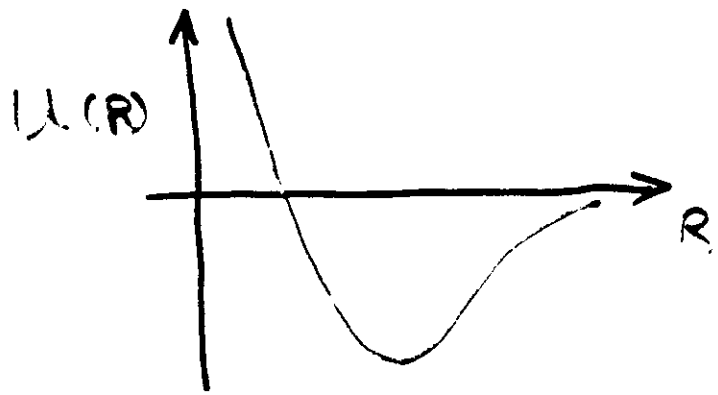

$$U(R) = \underbrace{E^{el}(R)}_{e^- \text{ binding energy}} + \underbrace{V^{nuc}(R)}_{\text{nuclear/nuc. repulsion}}$$

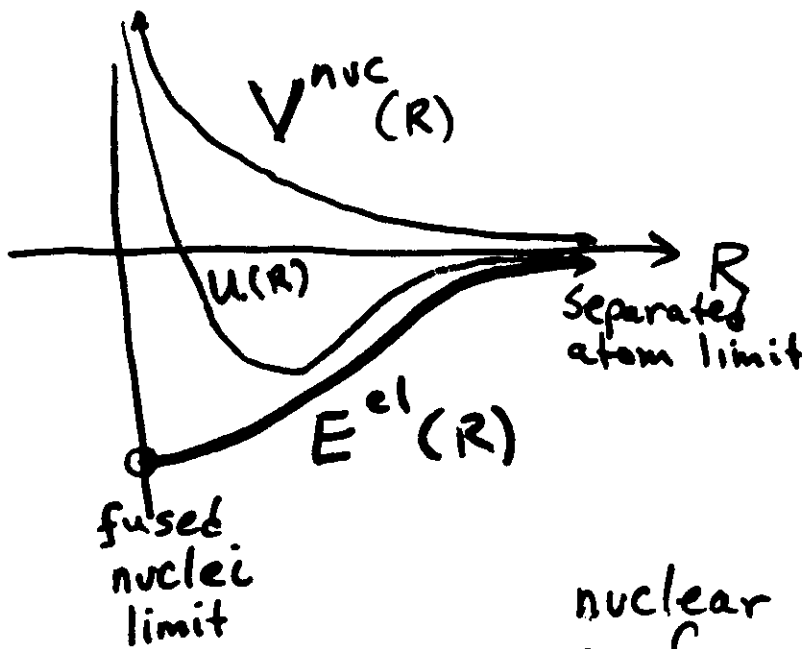

nuclear pot. energy surface

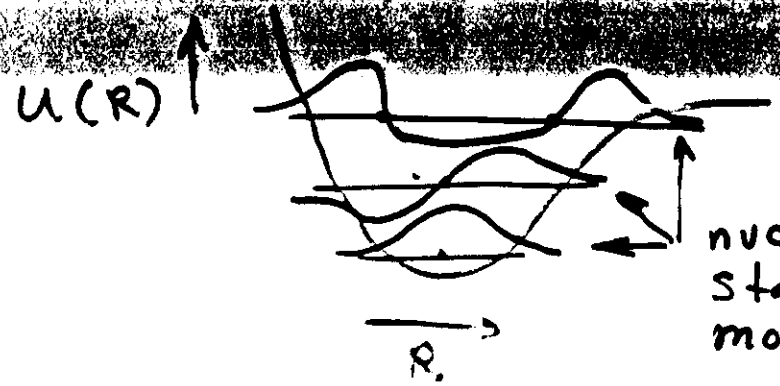

nuclear (vib.) states of molecules.

$$\Psi(r^{el}, R) \simeq \psi^{el}(r^{el}; R)\, \chi_n^{nuc}(R)$$

Born-Op. approx.

Vibronic Coupling ($T=0$) in the Context of optical absorption

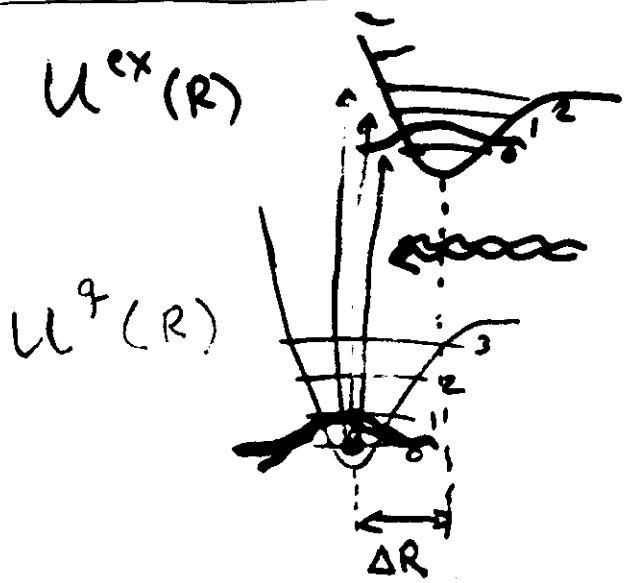

dipole perturbation

$H' = e\mathcal{E}\vec{r}$

connects $g \leftrightarrow ex$ surfaces

↳ reflects charge redistribution & nuc. geometry change.
(e.g. $\pi \rightarrow \pi^*$ transition)

$\int \psi^*(\epsilon) e^{ix} \psi(\epsilon)\, d\epsilon$

Prob. of transition $\propto \underbrace{\mu_{ge}^2}_{\text{electronic part}} \underbrace{\left| \int \chi_0^g(R)\, \chi_n^{ex}(R-R_0)\, dR \right|^2}_{\text{nuclear part}}$

$\frac{e^{-S} S^n}{n!}$

harmonic wells
$T = 0$
equal spring constants
k_e.

$S = \frac{\frac{1}{2} k_e \left(R^{e}_{equilib} - R^{g}_{equilib} \right)^2}{\frac{1}{2} \sqrt{\frac{k_e}{\mu}}} = \frac{\lambda}{\hbar\omega}$

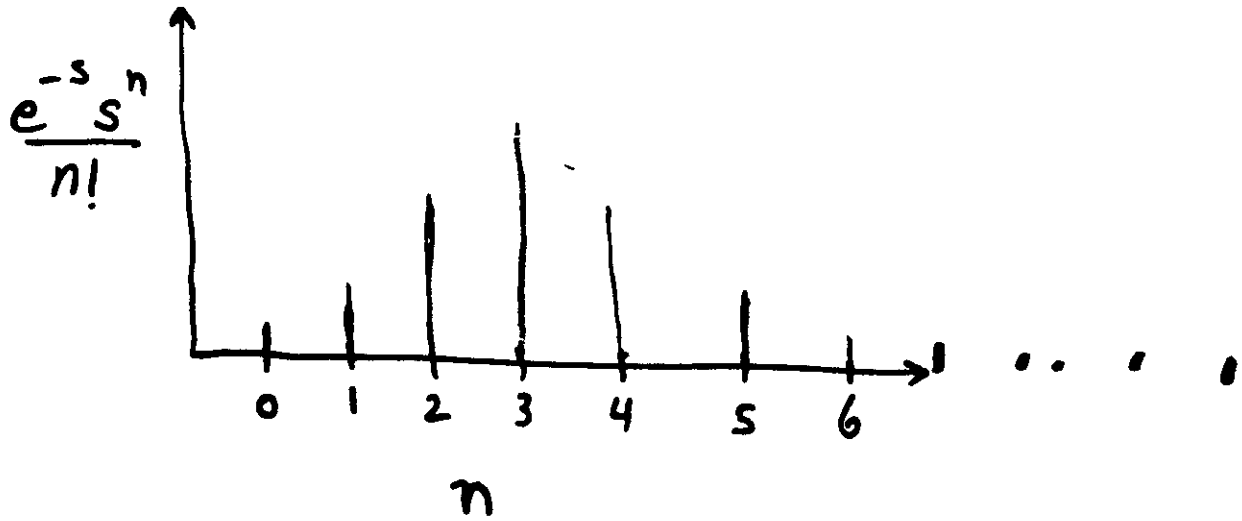

for $S = 3$

⊛ Why are optical spectra peaked ??

So: Opt. abs. spectrum ($g \rightarrow ex$) peak detd by e^- rearrangement.

why? $\int \chi_0' \chi_n^{ex} \, dR$ large for n where $\chi_0' \chi_n^{ex}$ is large:

$0 \rightarrow 0$  dR small

$0 \rightarrow 1$  dR larger

$0 \rightarrow 2$ 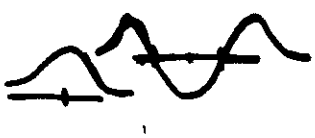 dR

$0 \rightarrow 3$ 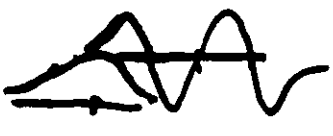 dR larger

$0 \rightarrow 10$ 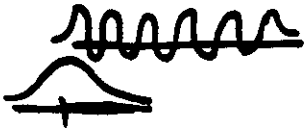 dR small

Intramolecular ET

In optical abs. e⁻ is redistributed

ET: extreme [illegible] e⁻ removal/insertion

D–A ⇒ D⁺A⁻

Process like opt. abs, but connection between wells is H' (to be discussed further!) not $e\vec{\mathcal{E}}\vec{R}$.

T=0, one mode

$$\text{Prob. (E.T.)} \propto H_{DA}^2 \left| \int \chi_0^{nuc}(R)\chi_n^{nuc}(R-R_0)dR \right|^2$$

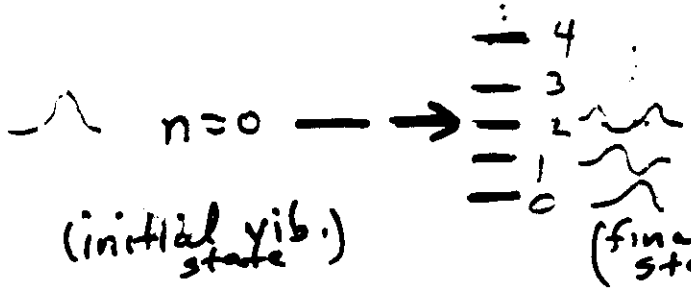

only 1 energy conserving transition

Useful picture for weak D/A cplg. regime.

$T = 0$, one mode:

$$n(\text{all have } \nu) = \frac{\Delta E^{rxn}}{\hbar\omega}$$

$$k_{DA \to D^*A} \propto \frac{e^{-S} S^n}{n!}$$

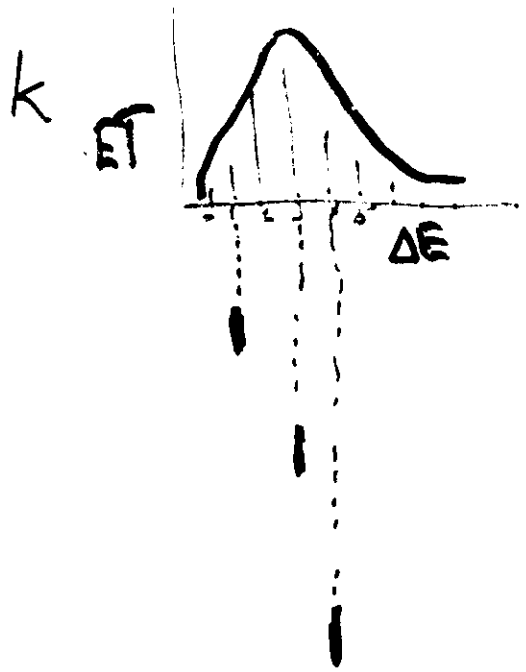

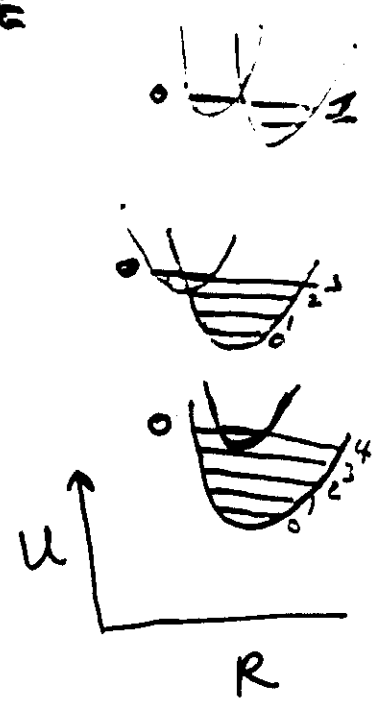

"normal"
$0 \to 1$ $\Delta E = \hbar\omega$

$0 \to 3$ $\Delta E = 3\hbar\omega$
"activationless"

$0 \to 4$ $\Delta E = 4\hbar\omega$
"inverted"

TWO-MODES &

IF $KT \gg \hbar\omega$ & keep simple rate

(also replace poissons with gaussians)

$$k_{ET} \propto \int \frac{1}{\sqrt{2\pi\sigma_D^2}} e^{-\frac{(E-E_D+\lambda)^2}{2\sigma_D^2}} \frac{1}{\sqrt{2\pi\sigma_A^2}} e^{-\frac{(E-E_A-\lambda)^2}{2\sigma_A^2}} dE$$

Prob. of removing e^- from D with energy E

Prob. of inserting e^- into A with energy E.

$\sigma(T)$

non-zero width because we can now leave behind different amounts of vib. energy.

Now,

normal activated regime (A)

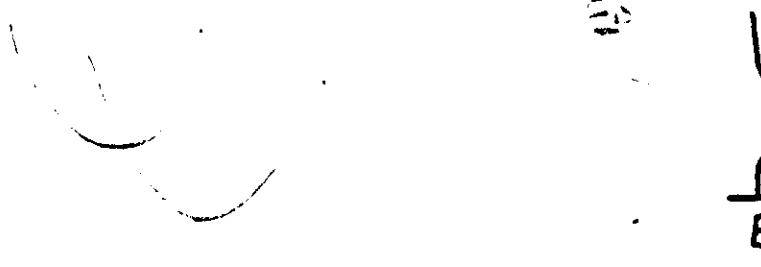

activationless (B)

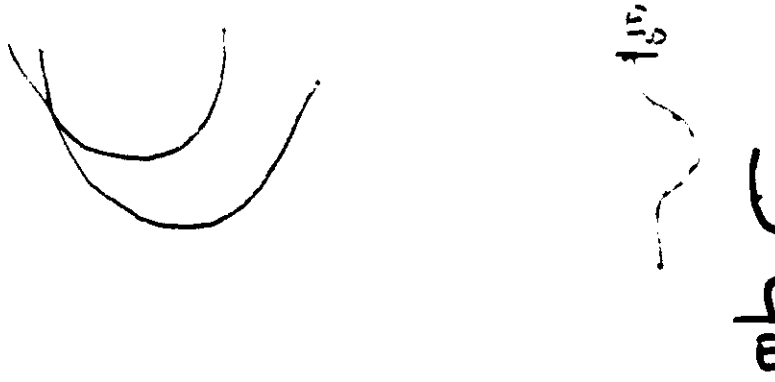

inverted regime (C)

qualitatively similar to T=0 view.

↳ Marcus Theory results

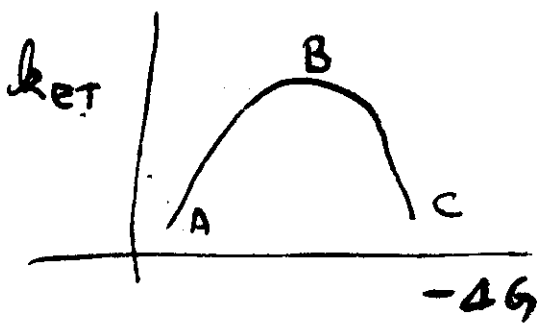

B. Electronic Dependence

$$k_{ET} \sim \left(\text{electronic coupling}\right)^2 \left(\text{nuclear factor}\right)$$

(** ** circled)

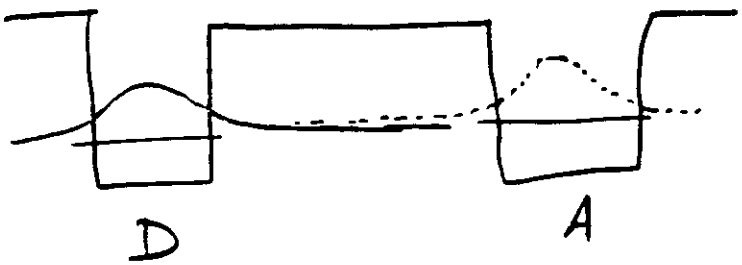

"Chemical" VIEW

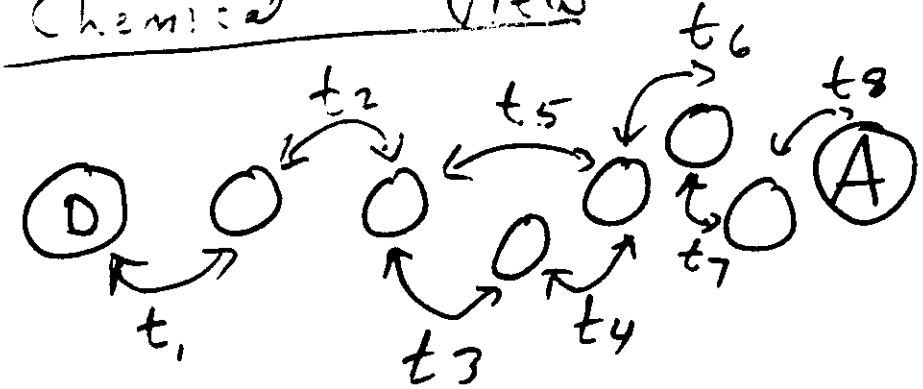

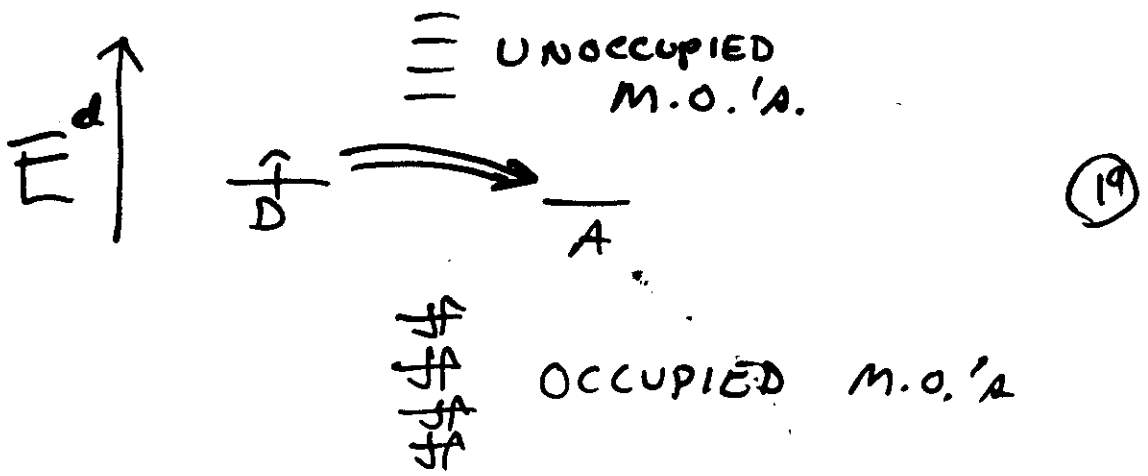

Decay of Coupling Across Covalent Bonds

ϵ = decay [illegible]

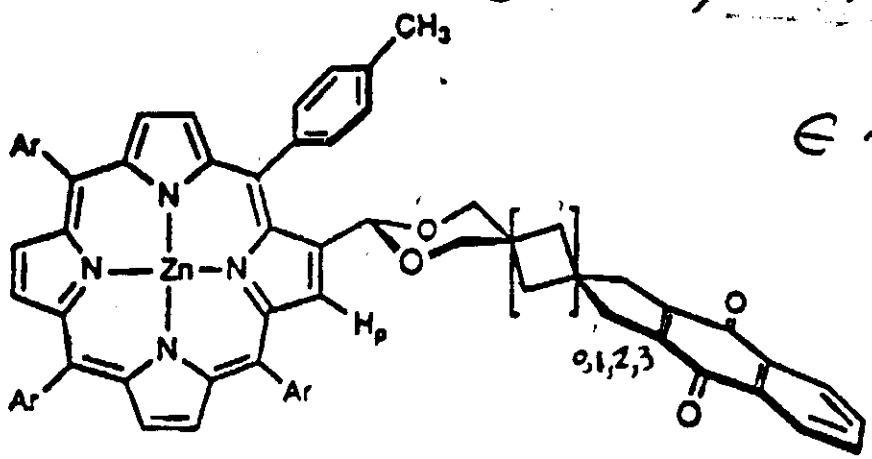

$\epsilon \sim .61$

Schuster et al.

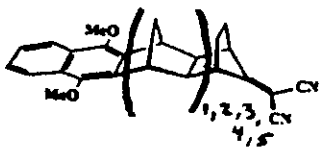

$\epsilon \sim .52 - .63$

Paddon-Row et al.

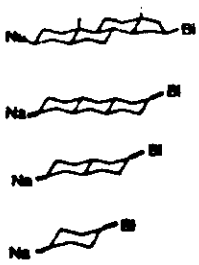

$\epsilon \sim .56$

Closs et al.

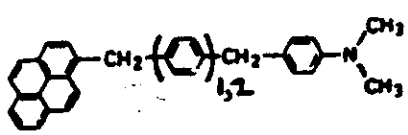

$\epsilon \sim .75$

Michel-Beyerle et al.

CLOSS + MILLER '86

TABLE II

Compound	Symbol	# of Bonds	# of Isom	Compt
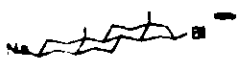	Ste	10	—	
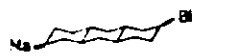	A-2,8	9	4	
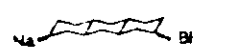	A-2,9	8	4	
	D-2,6	7	4	✓
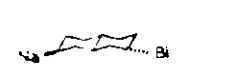	D-2,7	6	4	✓
	C-1,4	5	2	✓
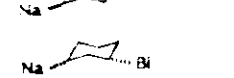	C-1,3	4	2	✓
	C-1,2	3	2	
	M	2	1	

TABLE III

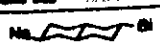	D-2,6-ee		D-2,7-ee
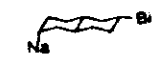	D-2,6-ea	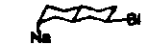	D-2,7-ea
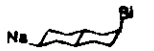	D-2,6-ae	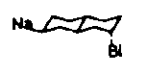	D-2,7-ae
	D-2,6-aa		D-2,7-aa

TABLE IV: Distances, Rate Constants, and Coupling Matrix Elements of Compounds with 4-Biphenyl-2-Naphthyl Donor–Acceptor Pairs

compd	$(R_{DA})_{center}$,[a] Å	$(R_{DA})_{edge}$,[a] Å	k,[b] s^{-1}	λ_v, eV	V, cm^{-1}
Ste	17.4	10.3	1.5×10^6	0.75	6.2
D-2,6					
ee	14.0	6.7	5.0×10^7	0.72	34
ea	11.4	6.3	5.9×10^7	0.67	26
ae	11.0	6.3	2.3×10^7	0.66	15
aa	11.9	6.1	5.8×10^7	0.68	27
D-2,7					
ee	12.5	6.4	2.9×10^8	0.69	63
ea	11.4	6.0	3.0×10^8	0.67	58
ae	10.9	6.0	1.75×10^8	0.66	42
aa	6.2	5.3	25×10^8	0.47	58
C-1,4					
ee	11.8	4.4	1.6×10^9	0.68	141
ea	9.5	4.0	2.5×10^9	0.62	129
ae	9.3	4.0	0.45×10^9	0.62	55
C-1,3					
ee	10.0	3.8	4.2×10^9	0.64	185

[a] Measured from distances optimized by molecular mechanics, MM-2 calculations. [b] Error limits estimated to be ±25%, and ±40% for rates in excess of 10^9 s^{-1}.

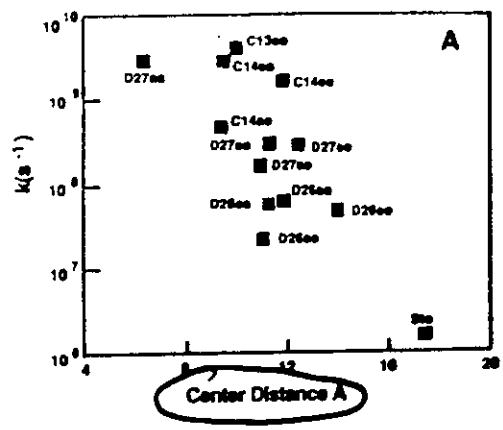

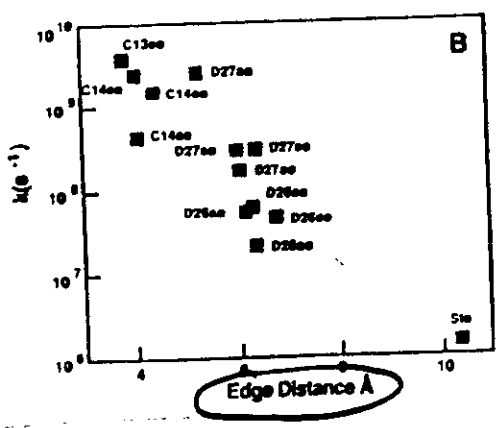

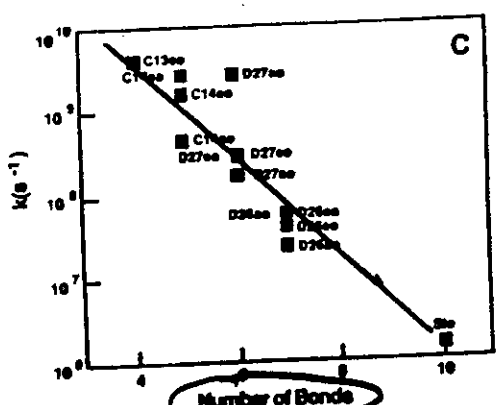

Figure 3. Intramolecular ET rates for the negative ions of the compounds listed in Tables II and III in THF at 296 K plotted against (A) center-to-center distance, (B) edge-to-edge distance, and (C) minimum number of intervening σ bonds.

$k_{ET} = e^{-\beta R}$

$\beta = 1.0\ Å^{-1}$ ✓

$\beta = 1.15\ bond^{-1}$

$e^{-1} = .37$

9)

21)

Intervalence bands & Coupling

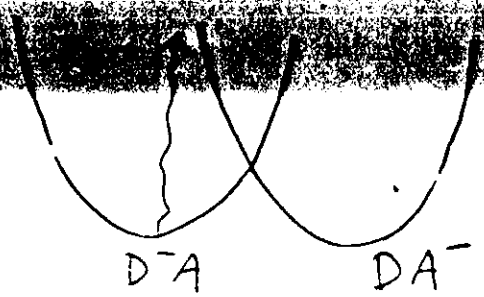

$E_{op} = \lambda$, strength of transition $\propto H_{DA}^2$

(Mulliken, Hush, etc.)

(weak coupling assumed)

$$H_{AB} = 2.05 \times 10^{-2}\left[\frac{\epsilon_{max}\Delta\bar{\nu}_{1/2}}{\bar{\nu}_{max}}\right]^{1/2}\frac{\bar{\nu}_{max}}{r}\ \text{cm}^{-1}$$

L—L	r, Å	λ_{max}, nm[a]	ϵ_{max}, M^{-1} cm^{-1}	$\Delta\bar{\nu}_{1/2}$(calc), kK	H_{AB}, cm^{-1}[b]
a_5Ru^{+2} 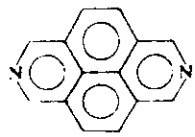 $Ru^{+3}a_5$	11.3	1000(10.3)	~1000	—	[400]
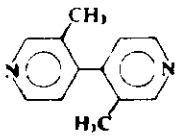	11.3	890(11.2)	165	6.2(5.1)	195
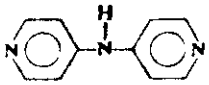	10.9	920(10.9)	1010	6.4(5.0)	500
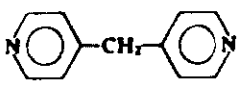	10.5	810(12.3)	30	7.1(5.3)	100
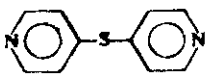	~11	855(11.7)	70	[7.3][c]	[~150]
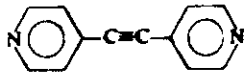	14.0	920(10.9)	640	5.4(5.0)	285
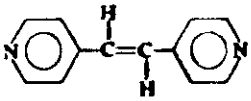	13.8	960(10.4)	760	5.3(4.9)	305
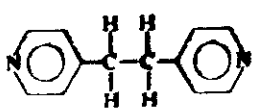	—	—	<10	—	—

D/A Coupling determined by D/A localized state propagation through bridge :

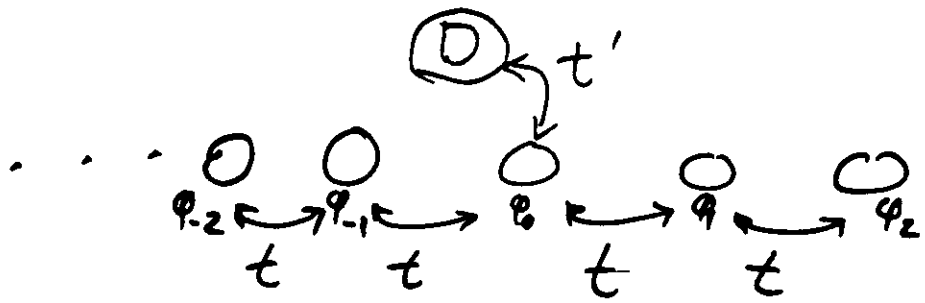

→ one orbital per bridge site

→ periodic bridge

→ $\psi_D \sim \sum_n \epsilon^{|n|} \varphi_n^{bridge}$

$$\epsilon + \frac{1}{\epsilon} = \frac{E}{t} \qquad \epsilon \simeq \left(\frac{t}{E}\right)$$ (2)

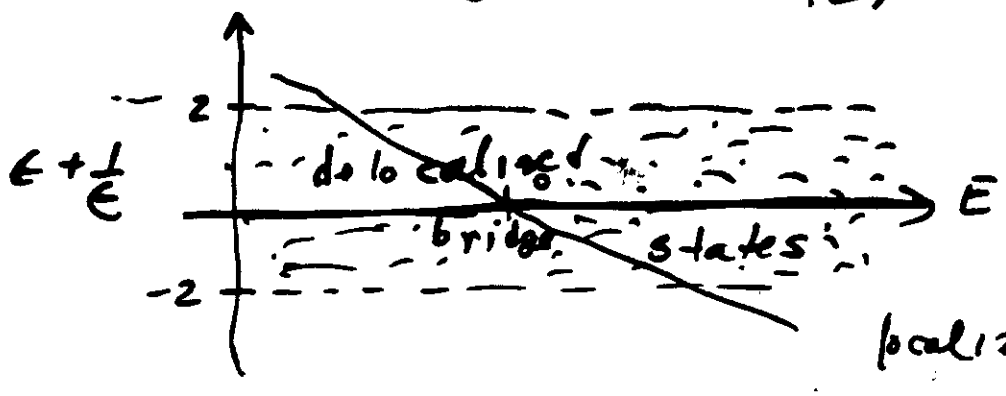

Here :

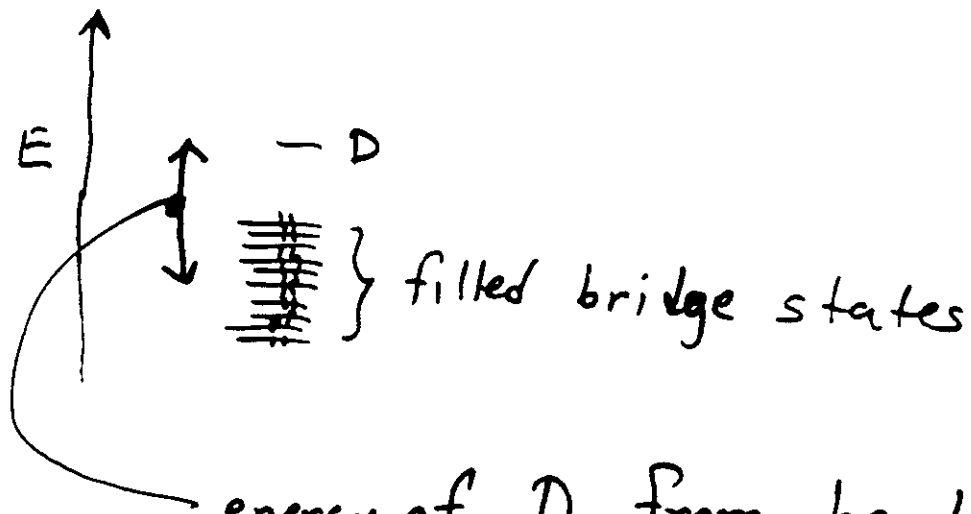

Typical values of $\epsilon \sim 0.6$ (per bond)

Typical Through-space decay

$$\sim \exp\left[-\sqrt{2m E_{bind}/\hbar^2}\, R\right]$$

$$\sim \exp\left[-1.7\, R\right] \quad \text{for } E_{bind} = 8eV$$

Through-bond decay quickly dominates !

Simple view of localized states in protein:

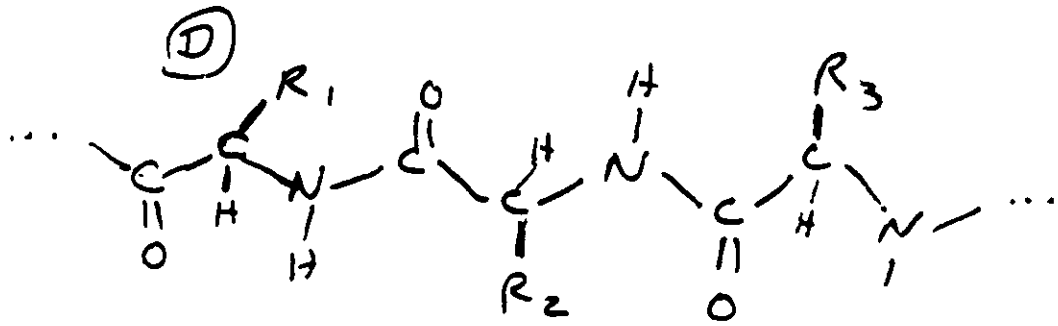

- define ϵ as <u>average decay of ψ_D per bond</u>.
- allow occasional (weak) through-space decay of ψ_D.

Size and complexity

Cytochrome *c*

~ 100 amino acids
~ 850 heavy atoms
~ 4500 valence electrons

- - - - - - - -

What level of theory is
predictive?
accessible?
warranted?

Electronic Coupling Models

1. Phenomenological Methods

Structureless Barriers: 1974-87

Hopfield
Jortner
⋮

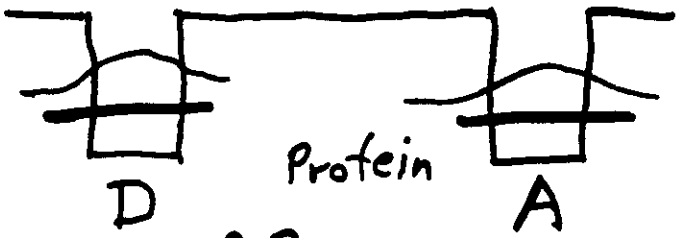

$$T_{DA}^2 = A e^{-\beta R_{DA}} \qquad R_{DA} \gtrsim 5\text{Å}$$

Structured barriers - Pathways: 1987–

Onuchic
&
[illegible]atan

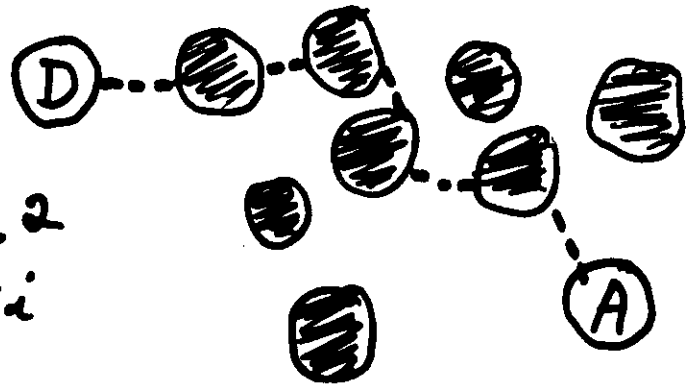

$$T_{DA}^2 = A \prod_{i=1}^{N} \epsilon_i^2$$

2. Quantitative Methods

Green's function strategies: 1991–

ersson
gama
ldman
atner
arcus
& B
⋮

$$T_{DA}^2 = (V_{DP} G_P V_{PA})^2$$

$$G_P = (H_P - E\mathbb{I})^{-1}$$

CRUX OF PROBLEM

Balancing by k_{ET} Interaction

* VACUUM TUNNELING *

$$T_{DA} \propto \exp\left[-\underbrace{\sqrt{2E_{BIND}}}_{1.7\text{Å}^{-1}} R_{DA} \right]$$

for $E_{BIND} = 8$ eV

FROM GAMOW 20's

* BOND MEDIATED TUNNELING *

$$T_{DA} \propto \exp\left[-\underbrace{\frac{1}{r_b}\left|\ell n \frac{\gamma}{E}\right|}_{0.6\text{Å}^{-1}} R_{DA} \right]$$

FROM MILLER & CLOSS 80's

If binding energies were only 1-2 eV, TB and TS coupling would be about equal.

and the problem would be trivial!!

****

PATHWAYS

C PLG.

$$\text{COUPLING} \propto \prod_i \epsilon_i$$

$$0 < \epsilon_i < 1$$

PHENOMONOLOGICAL MODEL...

... CALIBRATION

		MODEL
$\epsilon^{\text{COVALENT}} = 0.6$	:	COMPOUNDS
$\epsilon^{\text{H-BOND}} = (\epsilon^{\text{COVALENT}})^{\cdot}$	:	O-B '90
$\epsilon^{\text{SPACE}} = \epsilon^{\text{COVALENT}}\ \epsilon^{-1.7(R-R_0)}$	:	"Gamow"

MAXIMIZE $\left\{ \prod_i \epsilon_i \right\} \Rightarrow$ PATHWAY(S)
[BALANCES TB/TS CONTRIBS. TO T_{DH}]

MAPS ELECTRONIC STRUCTURE PROBLEM ONTO GRAPH THEORY PROBLEM...

ϵ's : RENORMALIZED PARAMETERS

(A)

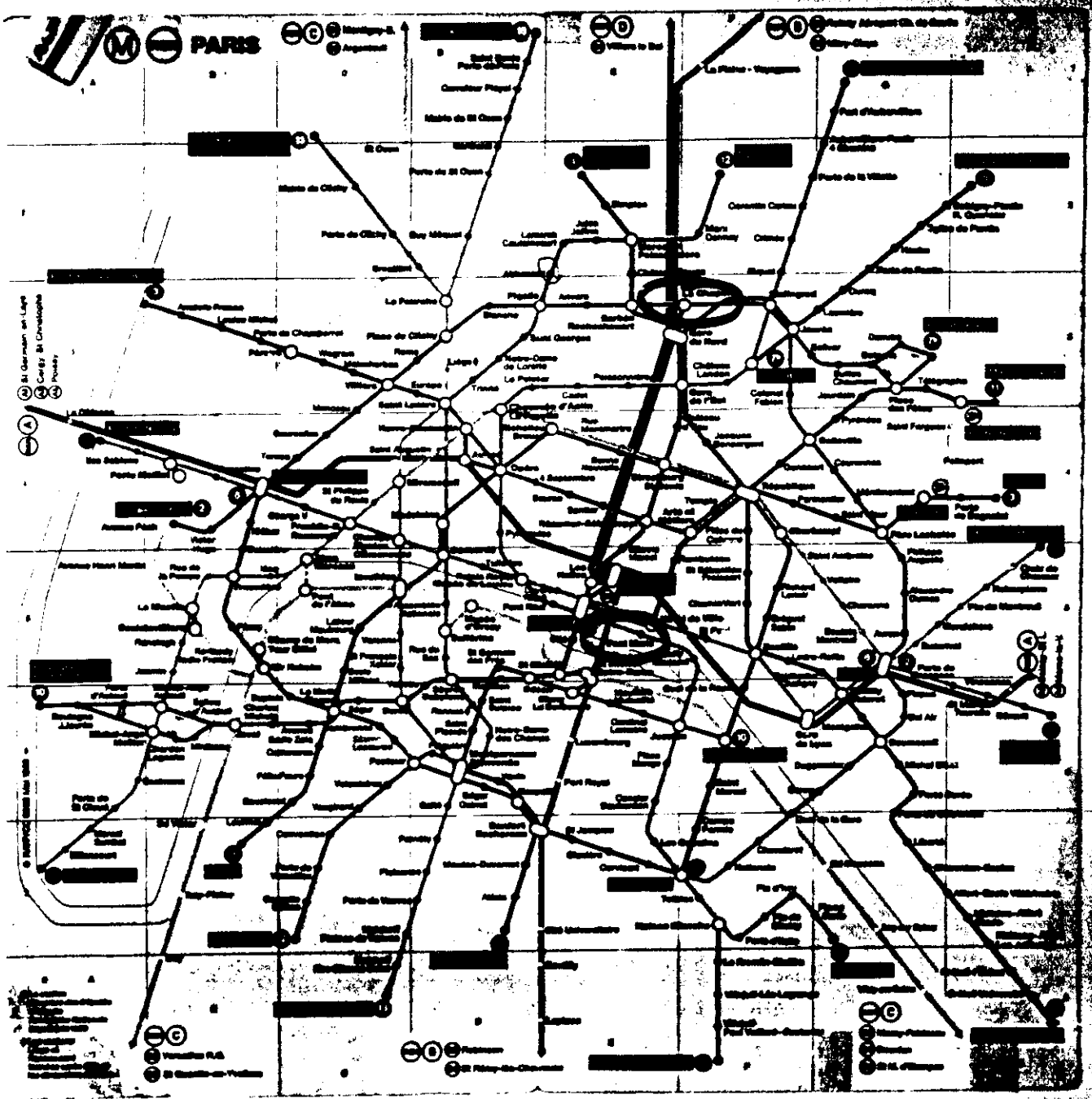

The minimum distance in a network or "graph" problem.

(T.S. cplg like a bus xsfr between lines)

Structural bridge models

⊛ β (through bond) $\sim 1.4\ \text{Å}^{-1}$

$\Rightarrow$

⊛ β (through space) $\sim 3.4\ \text{Å}^{-1}$

McConnell

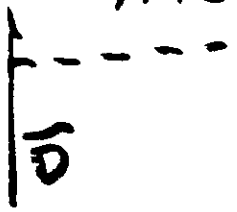

$$T_{DA} \propto \left(\frac{t}{E-\Delta}\right)^{n}$$

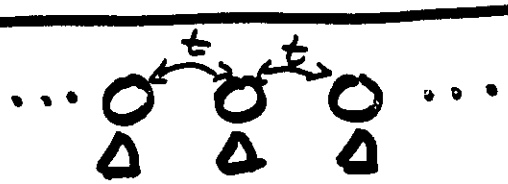

periodic 1D perturbation th.

generalized McConnell

$$T_{DA} \propto \prod_i \frac{t_i}{E-\Delta_i}$$

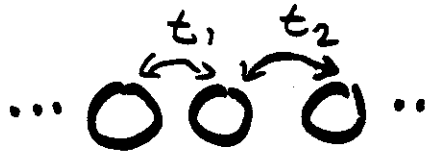

1D pert. th.

No loop bridge

$$T_{DA} \propto \prod_i \left(\frac{t_i}{E-\Delta_i-\alpha_i}\right)$$

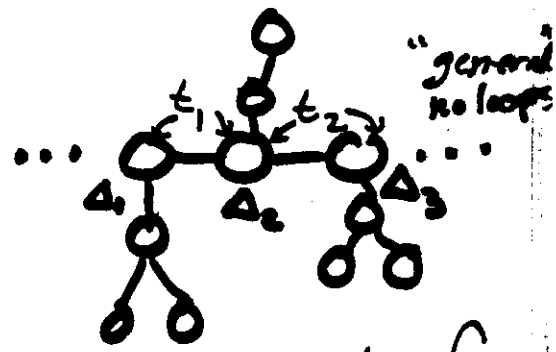

↑ reflects struct. of side chains

Pathways

$$T_{DA} \propto \frac{N_C}{\prod_{i=1}} \frac{N_S}{\prod_{j=1}} \frac{N_H}{\prod_{k=1}} \epsilon_i \epsilon_j \epsilon_k$$

no distinction between bond types (no loops)

(8)

k_{ET}

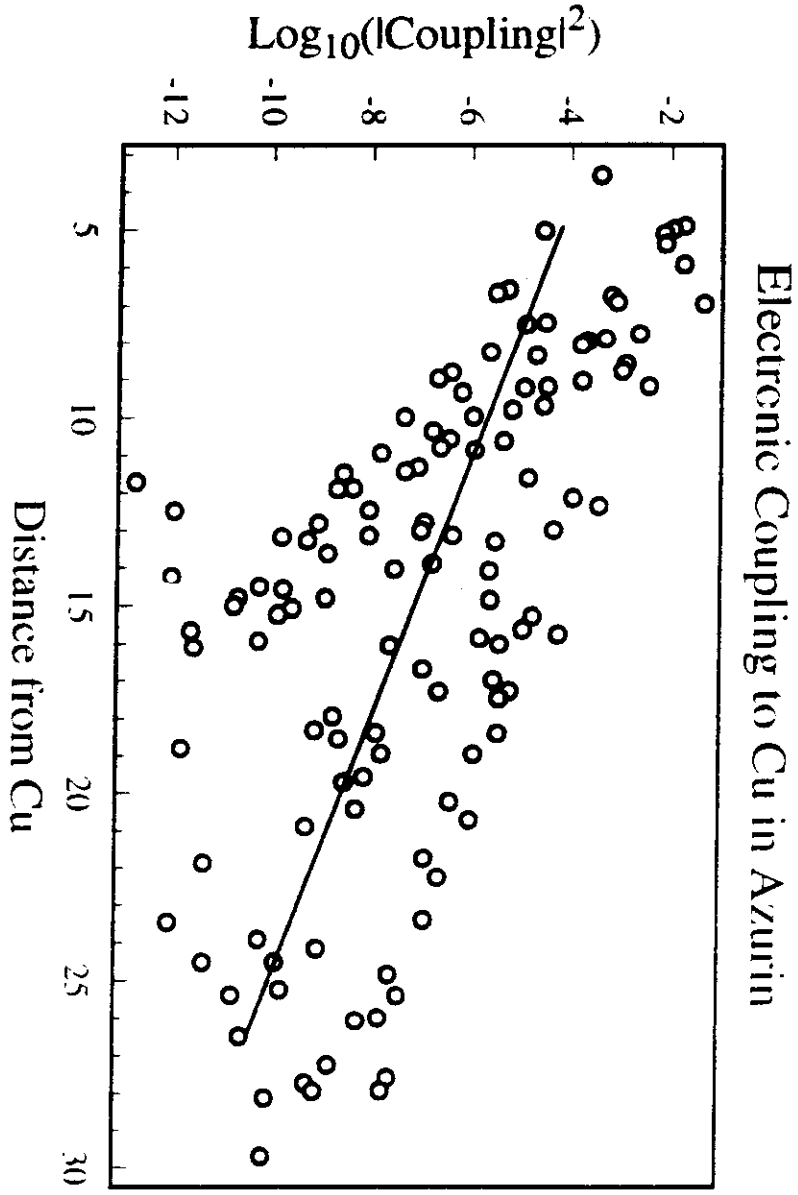
Log10(|Coupling|2)
-12
-10
-8
-6
-4
-2
5
10
15
20
25
30
Distance from Cu
Electronic Coupling to Cu in Azurin

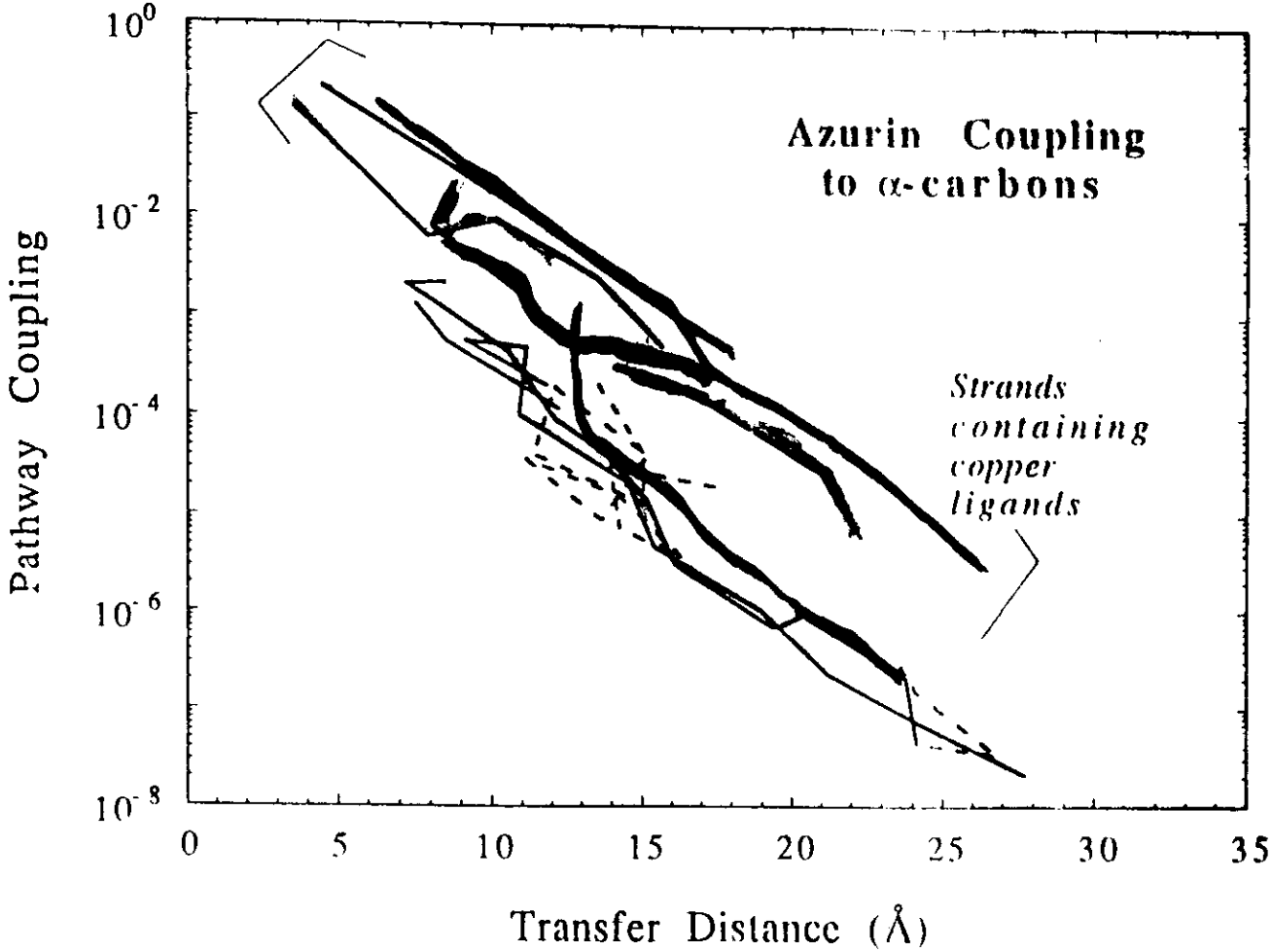
Azurin Coupling
to α-carbons
Strands
containing
copper
ligands
Pathway Coupling
10^0
10^-2
10^-4
10^-6
10^-8
0
5
10
15
20
25
30
35
Transfer Distance (Å)

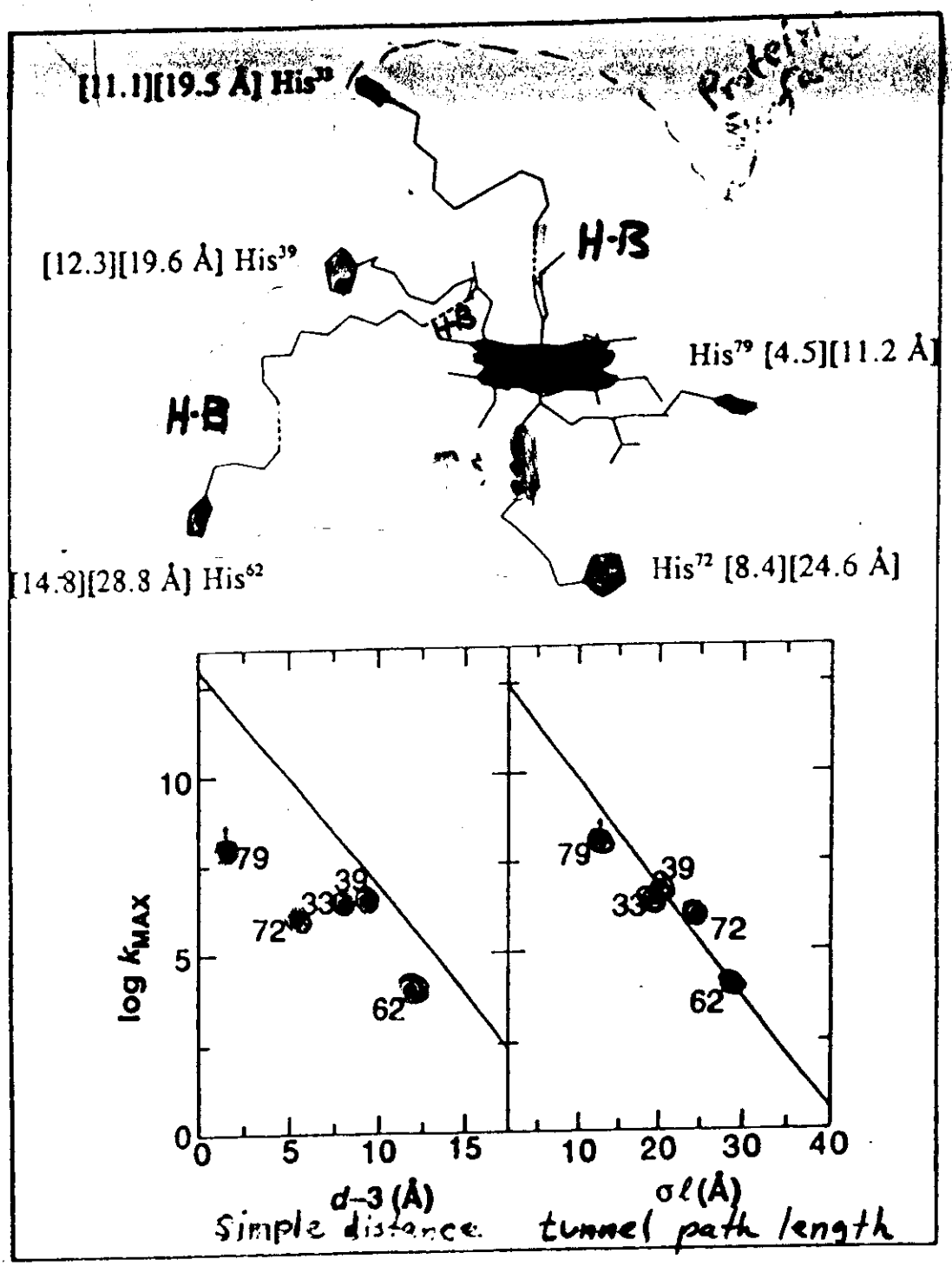

Fig. 1. (Upper) Electron-tunneling pathways in Ru(His^x)-modified cytochromes c (*2*). Edge-edge distances and tunneling path lengths are indicated in brackets ([d][$\sigma\ell$]). **(Lower)** Correlations of activationless ET rates in Ru(His^x)-modified cytochromes with d and $\sigma\ell$.

Applications of Pathway Method

cytc. KCP

Pellitier and Kraut

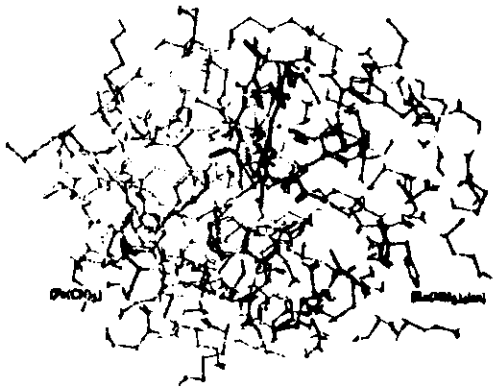

cyt. C

Isied

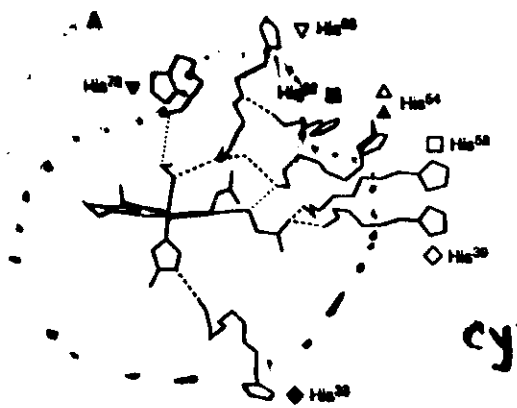

cyt.C

Gray

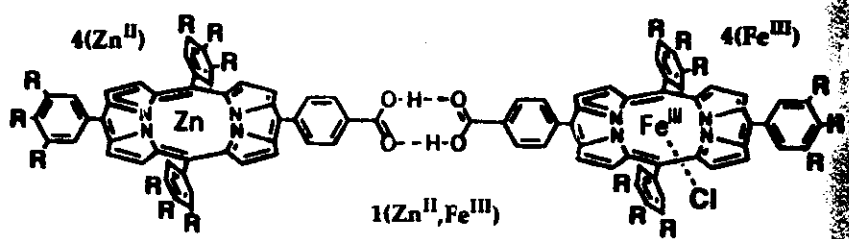

Therien

Average decay factors: $T_{DA} \propto \exp\left[-\frac{\beta}{2} R_{DA}\right]$

PROTEIN	$\beta/2$ FIT	% helix	% Sheet
cytochrome c_{551}	0.8 $Å^{-1}$	51	-
myoglobin	0.7 $Å^{-1}$	79	-
cytochrome b_5	0.7 $Å^{-1}$	51.	29
cytochrome c	0.6 $Å^{-1}$	51	-
HIPIP	0.6 $Å^{-1}$	11	16
azurin	0.5 $Å^{-1}$	14	47
plastocyanin	0.5 $Å^{-1}$	5	62

H-BOND PATTERNS

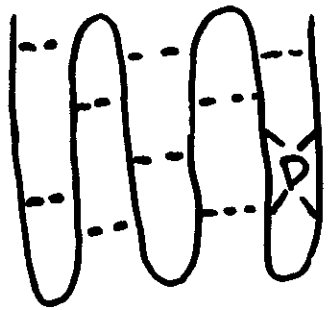

β- SHEET

ACCESSIBILITY WITHIN AND BETWEEN STRANDS

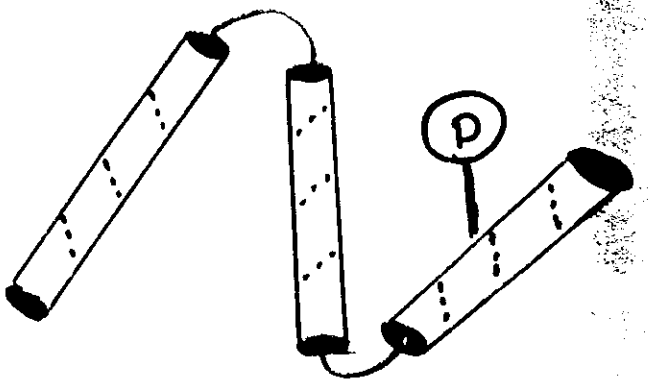

α - HELIX

ACCESSIBILITY WITHIN BUT NOT BETWEEN STRANDS.

Gray & co-workers: Ru-proteins

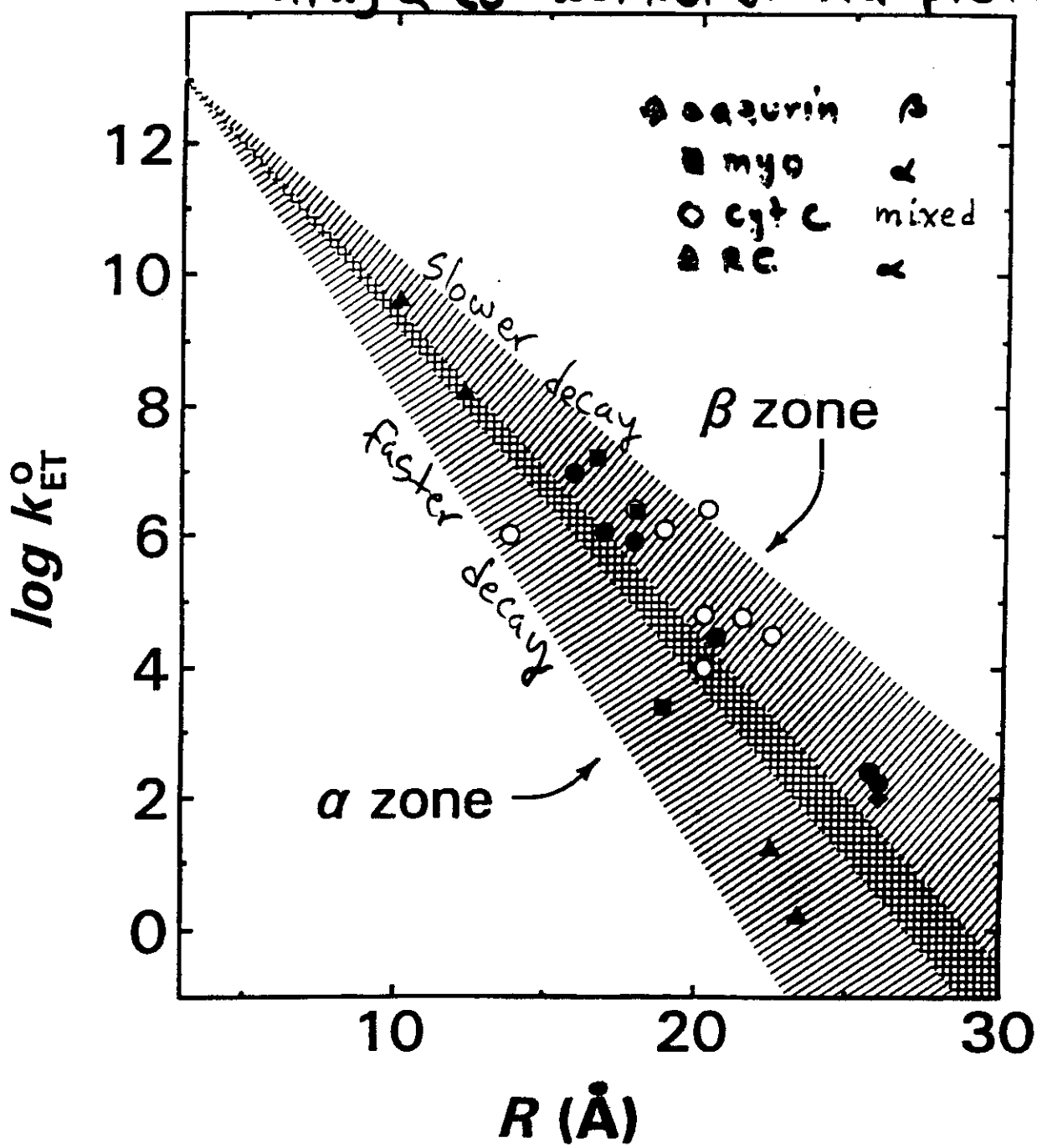

What do simple models lack?

1. **Pathway interference that arises from 2° and 3° structure.**
2. **Atom and bond type differences.**
3. **Donor and acceptor electronic structural details.**
4. **Dissection of coupling paths into relative contributions overall and into electron/hole components.**
5. **Independent electron models get energy scale qualitatively wrong.**

$$D^{-}PA \xrightarrow{DP^{-}A \text{ and } D^{-}P^{+}A^{-}} DPA^{-}$$

6. **Dynamics!**

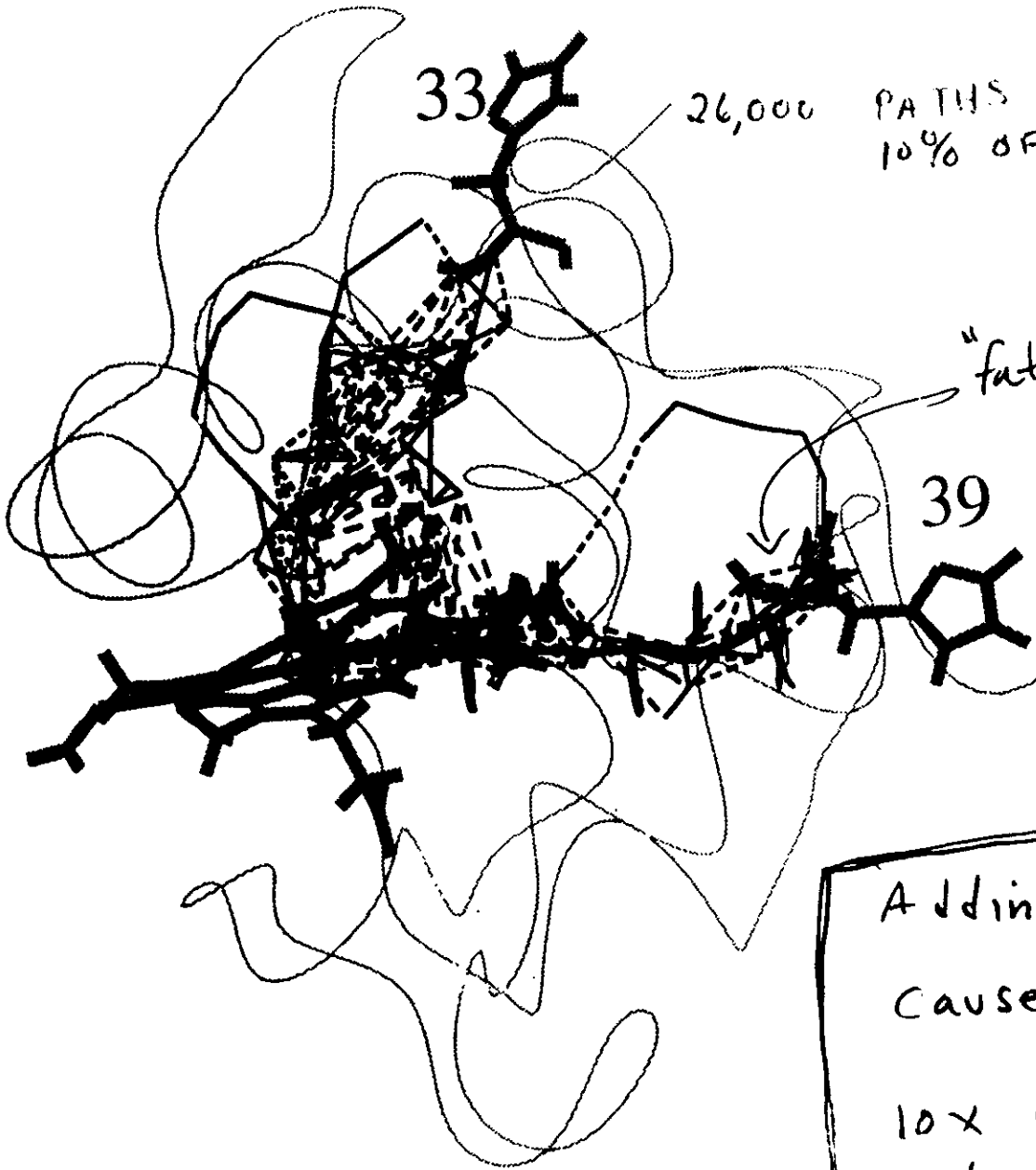

Adding ALL paths
Causes at most

10x change over
cplg thru "flatten
best path (GIN

Orbital Energetics:

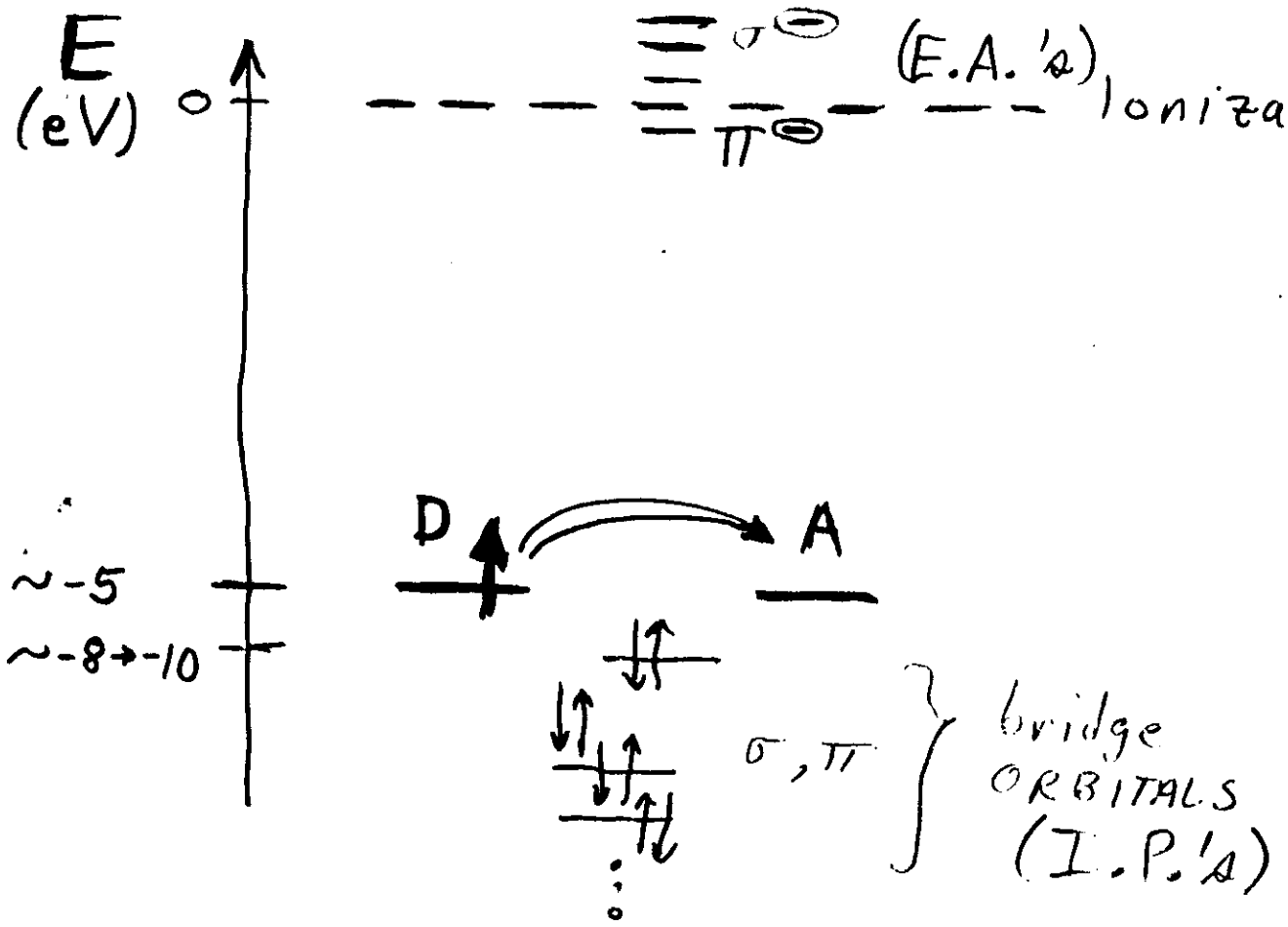

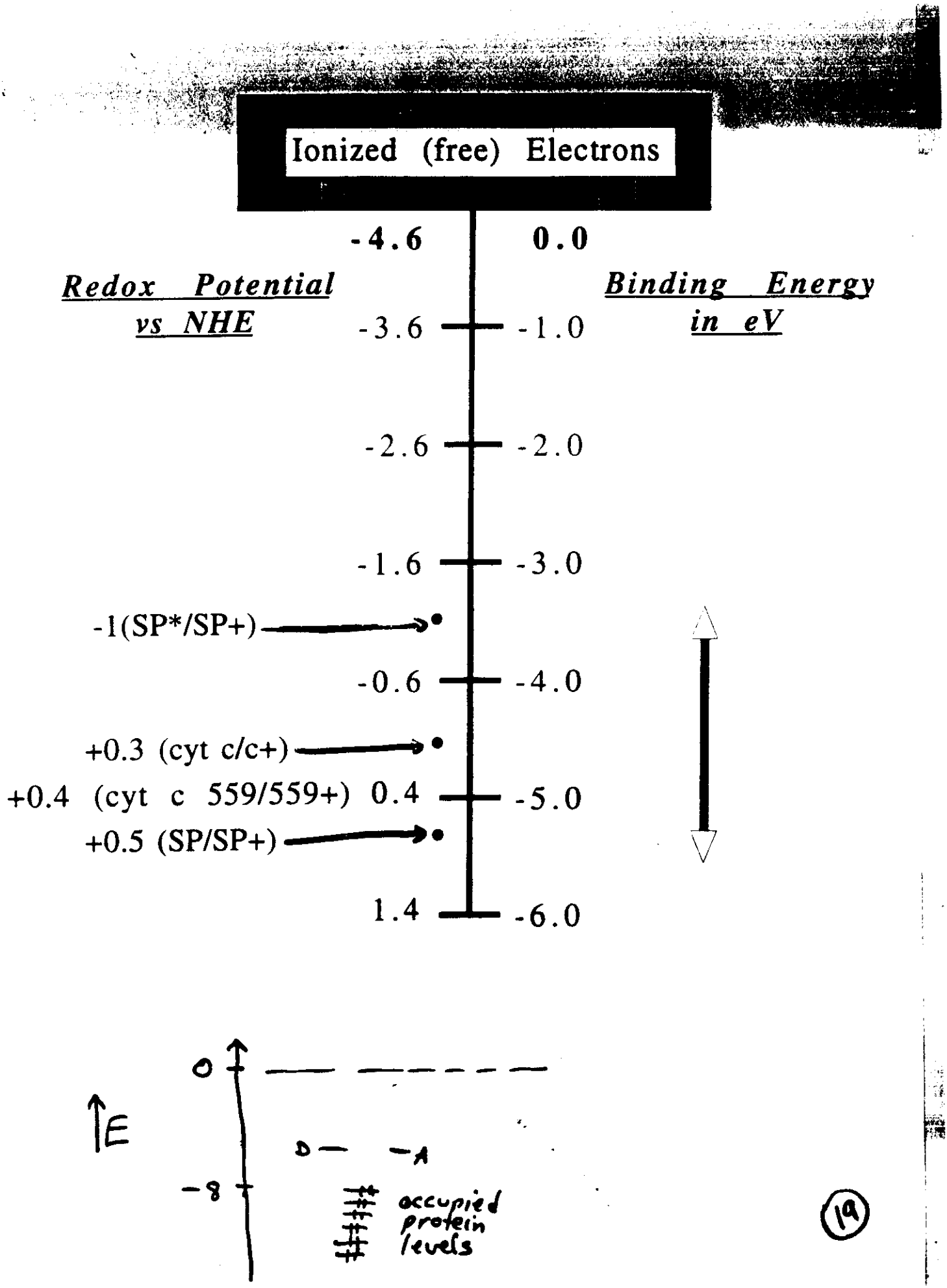
Ionized (free) Electrons
-4.6
0.0
Redox Potential vs NHE
Binding Energy in eV
-3.6
-1.0
-2.6
-2.0
-1.6
-3.0
-1(SP*/SP+)
-0.6
-4.0
+0.3 (cyt c/c+)
+0.4 (cyt c 559/559+) 0.4
-5.0
+0.5 (SP/SP+)
1.4
-6.0

0
E
D
A
-8
occupied protein levels

Electronic propagation

D^- ••• B1 B2 B3 B4 ••• A

D ••• B1 $B2^-$ B3 B4 ••• A

D ••• $B1^-$ B2 B3 B4 ••• A

D ••• B1 B2 B3 $B4^-$ ••• A

D ••• B1 B2 B3 B4 ••• A^-

••• + •••

Hole propagation

D^- ••• B1 B2 B3 $B4^+$ ••• A^-

D^- ••• $B1^+$ B2 B3 B4 ••• A^-

D ••• B1 B2 B3 B4 ••• A^-

$E(Bn^{+/-})$ not $E(Bn)$ relevant

⇑ anion/cation bridge states

⇑ neutral bridge states

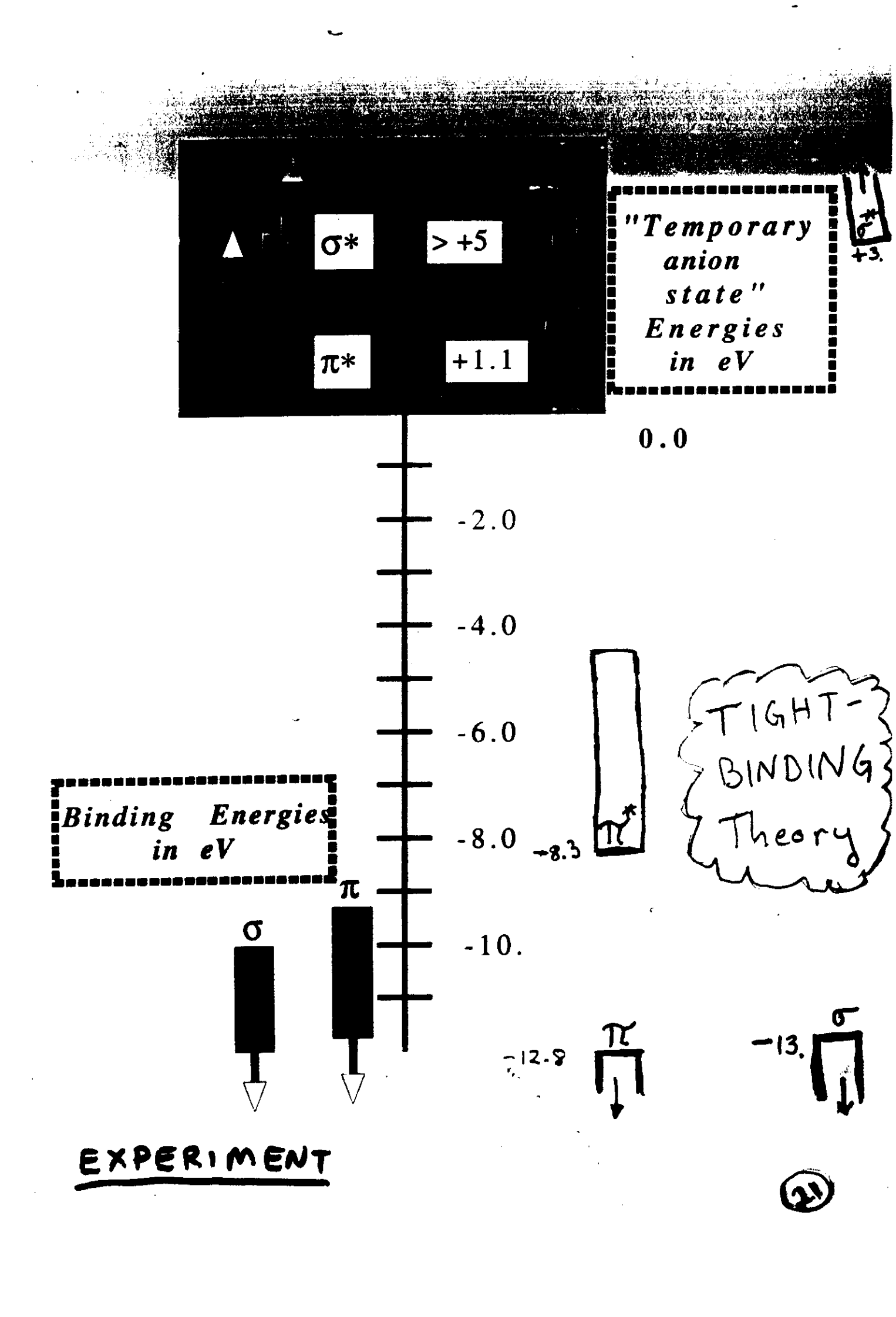
σ*
> +5
π*
+1.1
"Temporary anion state" Energies in eV
+3.
0.0
-2.0
-4.0
-6.0
-8.0
-10.
Binding Energies in eV
π
σ
-8.3
π*
TIGHT-BINDING Theory
-12.8
π
-13.
σ
EXPERIMENT
21

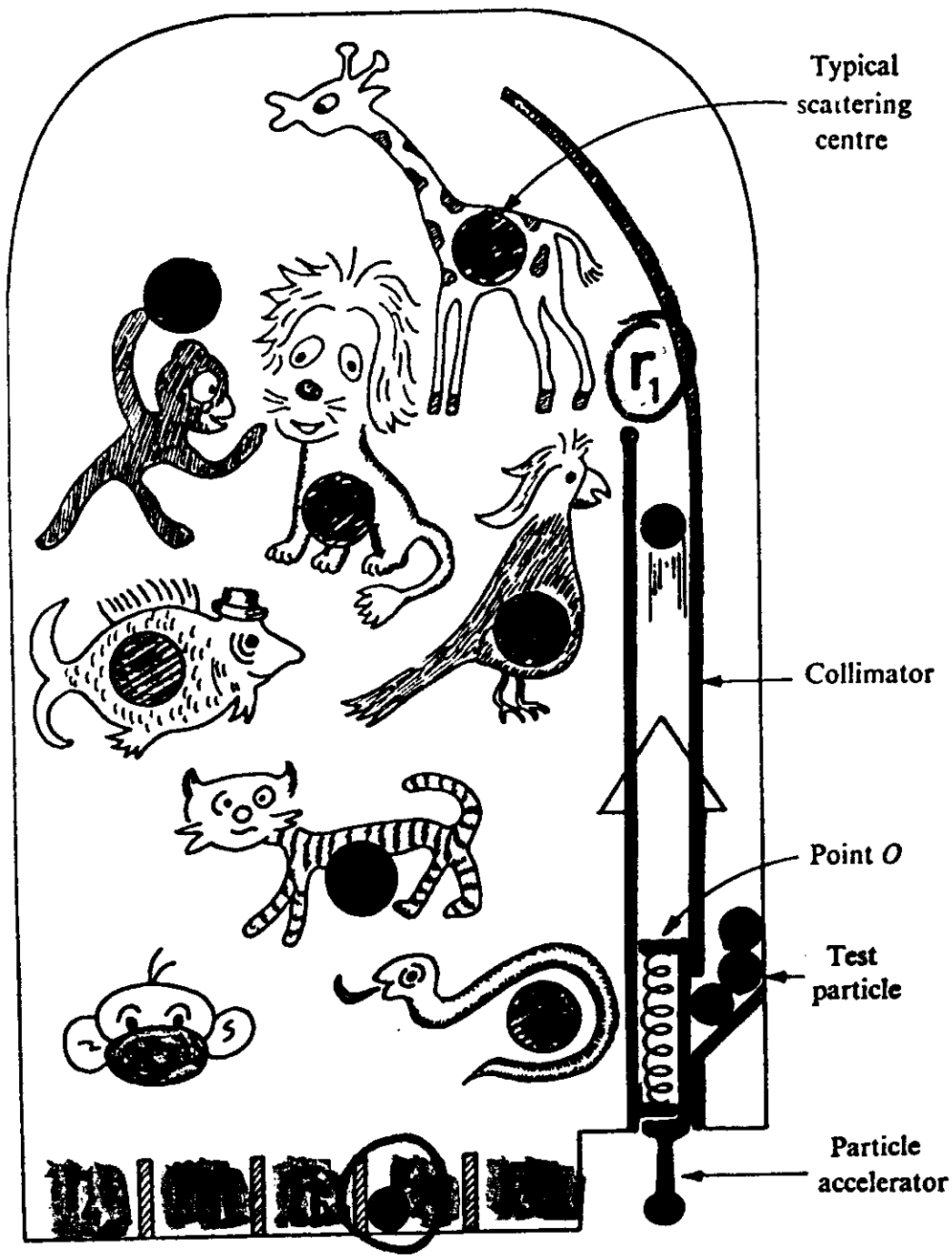
Typical scattering centre
r_1
Collimator
Point O
Test particle
Particle accelerator

Total prob. of going from r_1 to r_2

SUM OVER ALL POSSIBLE PATHWAYS

D / Protein / A Hamiltonian

$$H = \begin{bmatrix} H_D & V_{DP} & H_{DA} \\ V_{PA} & H_P & V_{PA} \\ H_{AD} & V_{AP} & H_A \end{bmatrix}$$

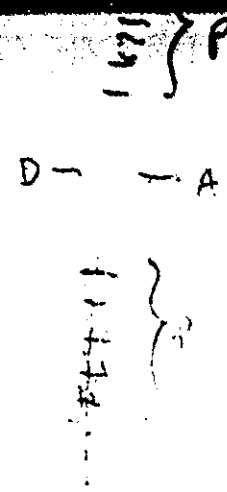

Two-level reduction

$$H\ (E) = \begin{bmatrix} [H_D + V_{DP}(E - H_P)^{-1} V_{PD}] & [H_{DA} + V_{DP}(E - H_P)^{-1} V_{PA}] \\ [H_{AD} + V_{AP}(E - H_P)^{-1} V_{PD}] & [H_A + V_{AP}(E - H_P)^{-1} V_{PA}] \end{bmatrix}$$

G → eff. coupling

$$\left(\begin{matrix}\text{effective}\\ \text{cplg. element}\end{matrix}\right) = \sum_n \left(\frac{V_{Dn}\, V_{nA}}{E - \mathcal{E}_n}\right)$$

$$V_{Dn} = \langle \varphi_D | V | \varphi_n \rangle$$

$$V_{nA} = \langle \varphi_n | V | \varphi_A \rangle$$

$\mathcal{E}_n$ = n^{th} molecular orbital energy of protein.

$$\text{cplg} = \sum_{n_{\text{occupied}}} \frac{\quad}{\quad} + \sum_{n_{\text{unoccupied}}} \frac{\quad}{\quad}$$

To appear as Chapter 2 and Appendix A in *Protein Electron Transfer*, D. Bendall editor, Bios Scientific Publishers, Oxford.

Chapter 2: The protein bridge between redox centers

David N. Beratan[1] and José Nelson Onuchic[2]

[1] *Department of Chemistry, University of Pittsburgh, Pittsburgh, PA 15260*
[2] *Department of Physics, University of California, San Diego, La Jolla, CA 92093*

2.1 Introduction.

The unifying theme of the electron transfer (ET) processes discussed in this book is motion of a single electron from one center of localization (chlorophyll special pair, heme, blue copper center, flavin, tyrosyl radical, etc.) to another one that is separated in distance by several angstroms (Lippard and Berg, 1994; Bertini *et al*, 1994). Furthermore, the centers (in most cases) are insulated from one another. The electrons that are being shuttled, whether photoexcited or not, propagate from donor to acceptor without forming real long-lived intermediate (reduced or oxidized) protein states (Hopfield, 1974). That is, the protein is not acting as a conductor or a photoconductor. As we shall see, the ET reactions of interest involve long range tunneling between localized D and A states that fall (energetically) within the HOMO-LUMO gap of an otherwise insulating material.

What tunnels?

The deVault-Chance experiment first demonstrated, and later experiments confirmed,

that long distance electron transfer reactions are viable from room temperatures to cryogenic temperatures (DeVault, 1984). Insensitivity to temperatures is the signature of activationless processes and/or tunneling. Two types of motion are associated with electron transfer: motion of the electron itself from donor to acceptor and nuclear motion associated with readjustment of protein and solvent nuclei to the electron redistribution of the oxidation/reduction event. The nuclear rearrangement involves high frequency inner sphere modes (covalent bonds of the donor and acceptor) as well as outer sphere modes (protein and solvent) that adjust to the charge redistribution. While most of this chapter deals with single electron transfer processes, much of biology relies upon coupled multi-electron and proton-coupled electron transfer. Our understanding of these coupled processes is less well developed than that of the single electron process.

In most electron transfer reactions of interest, electrons flow between redox active cofactors in protein: blue copper centers, hemes, iron-sulfur clusters, chlorophylls, etc. Aromatic amino acid side chains occasionally act as electron donors or acceptors, usually in the presence of a highly reactive redox partner. Oxidized or reduced amino acid intermediates do not form in most ET reactions. As such, true intermediate oxidized/reduced states of the protein do not exit. The energy needed to form such intermediates far exceeds thermal energies, K_BT. Since the donor and acceptor are not in direct contact, the electron must tunnel to move from donor to acceptor. Thus, in the long distance electron transfer reactions of interest in this book the dynamics is dominated by electron tunneling; the nature of the nuclear motion (classical or quantum) will depend upon the specific system. To describe the electron tunneling further, we need to consider the strength and the nature of the electronic interactions between donor and acceptor imbedded in the protein as well as the vibronic coupling.

Strong vs. weak electronic coupling regimes

Most biological ET reactions involve donors and acceptors that interact weakly and the reactions are nonadiabatic. As such, the ET reaction rate depends upon both an electronic interaction and a term associated the nuclear barrier (DeVault, 1984; Sutin and Marcus 1985). In contrast, ET between donor and acceptor species in direct contact and strong communication with one another is controlled by nuclear motion, as electronic interactions are so strong that they cease to control the reacton rate. This may be the relevant regime for exchange of electrons between proteins and other small mobile reactants (e.g., inorganic complexes) but seems to be of limited physiological importance. Most biological ET reactions seems to involve reactant cofactors imbedded within proteins.

The protein provides steric constraints that prohibit the reactants to contact one another directly, leading to the weak interaction nonadiabatic regime.

Rates of nonadiabatic ET can be written

$$k_{ET} = \frac{2\pi}{\hbar}|T_{DA}|^2(F.C.) \tag{2.1}$$

The reaction free energy dependence is contained in the Franck-Condon factor (F.C.). Effects associated with nuclear tunneling and with thermally activated barrier crossing are contained in this factor. T_{DA} describes the donor-acceptor interaction associated with electron tunneling.

Physical systems are most readily described in terms of their Hamiltonian, that is the sum of their kinetic and potential energies. For quantum systems, the classical quantities are replaced by operators. The small energy of interest, T_{DA}, does not appear explicitly in the Hamiltionian of the system. Methods to manipulate the hamiltonian in order to compute T_{DA} are described in section 2.3 and in Appendix A.

The non-adiabatic electron transfer rate in eq. 2.1 is valid in the weak interaction regime, i.e., the matrix element T_{DA} is very small. We now discuss what we mean by small. Appendix A shows that the electron can only tunnel between the donor and acceptor sites when their energies are resonant. That happens at particular reaction coordinate geometries that modulate the electronic energies of the donor and acceptor. The question becomes how long does this degeneracy last compared to the resonant donor-acceptor electron hopping frequency ($T_{DA}/\hbar$) once this resonance is achieved? If the system stays resonant for times short compared to this electronic oscillation time, the non-adiabatic limit is valid. In the opposite limit, the rate is adiabatic. This description is very intuitively appealing, but is not entirely complete. A quantum description of these issues should be consulted for more details (Onuchic and Wolynes, 1988).

In the case of an overdamped harmonic reaction coordinate (see appendix A), the resonance time can be calculated analytically. Resonance occurs exactly at the crossing point of the donor and acceptor surfaces (Marcus parabolas). The resonance time is therefore the time that the system takes to drift away from this crossing point:

$$t_{drift} = \frac{2T_{DA}}{\lambda\omega_c}. \tag{2.2}$$

λ is the reorganization energy and $\omega_c = \omega^2/\eta$ is the overdamped frequency. The complete expression for the electron transfer rate is then

$$\frac{2\pi}{\hbar}|T_{DA}|^2 \frac{1}{1 + 2\pi|T_{DA}|^2/\hbar\omega_c\lambda}\ (F.C.). \tag{2.3}$$

Clearly, when $t_{drift} \ll \hbar/T_{DA}$, the non-adiabatic limit is valid.

This overdamped limit is particularly interesting because it is mathematically equivalent to a Debye-like model for polar solvents. The reaction coordinate in this case is the total polarization coupled to the transfer electron. The polarization dynamics of a Debye solvent is equivalent to that of an overdamped harmonic oscillater. The coupling of this solvent to the electron transfer rate is obtained by replacing ω_c by τ_L^{-1}. $\tau_L = \tau_D/\epsilon_0$ (Garg *et al*, 1983; Zusman, 1994; Calef and Wolynes, 1983).

Tunneling electrons

What is the meaning of T_{DA} in the ET rate equation? In the hydrogen molecule ion, the energy splitting between the σ and σ^* orbitals can be associated with an oscillation frequency, $\omega = \Delta E/2h$. That is, if an electron is started out on the left-hand atomic orbital, its probability of being found on the left orbital at a later time oscillates as $\cos^2 \omega t$. In the more general case of donor and acceptor separated from one another by a bridge consisting of many thousands of orbitals, we need to compute the frequency of exchange between donor and acceptor. Here too, the frequency which we call T_{da}/h is associated with a splitting, but the splitting arises from the donor-acceptor interaction provided by the presence of the intervening and surrounding protein orbitals. The formal procedure to calculated this mediated splitting, or coupling, lies at the heart of the protein ET problem (some details of this procedure are discussed in the appendix). Defining the effective two state problem and estimating the associated splittings has occupied numerous groups over the last several years. Simple approximations to this splitting are estimated with our Pathway methods; numerical methods that deal explicitly with multiple interfering paths utilize Green function or path integral techniques. At the present time, it appears that the remaining bottleneck is not our ability to perform the splitting computation itself for thousands or orbitals, but rather to build a meaningful effective Hamiltonian for the protein ET problem.

Basics of vibronically coupled electron tunneling

Electrons tunnel in biological systems because thermal energies (K_BT = 1/40 eV at room temperature) are much smaller than the energies needed to promote an electron from the donor onto the bridge or from the bridge onto the acceptor. Nuclei, however, may tunnel or move classically depending upon the nuclear barrier to reaction. Formulation of the nonadiabatic electron transfer rate usually relies upon a Born-Oppenheimer/Franck-Condon formulation. These approximations are discussed in Appendix A. Usually, a frozen nuclear geometry is assumed for the protein in which the electron tunneling inter-

action between donor and acceptor is to be computed. What does this mean?

The donor and acceptor localized states must be brought into degeneracy or near degeneracy in order for the electron to tunnel (Hopfield, 1974; deVault, 1984; Sutin and Marcus, 1985). Electronic energy (binding energy, in eV for example) can be associated directly with a redox potential (Bard and Faulkner, 1980). So the problem of electron tunneling in proteins is one of electron tunneling in nuclear geometries around the "activated complex" structure. This geometry differs in that nuclei around donor and acceptor have begun to adjust to accomodate the change in charge associated with oxidation of D and reduction of A. If modes with similar frequencies and couplings exist on donor and acceptor, a useful approximation to the tunneling energy is derived from the average redox potentials of D/D^+ and A/A^- (Onuchic *et al*, 1986). In some cases, the donor-acceptor interaction may be hypersensitive to nuclear coordinates and the Condon approximation may not be appropriate. A near degeneracy with a bridge state or an *extremely* long distance transfer event event may complicate the Condon approximation.

The electronic portion of the protein ET problem, then, is one of an electron with tunneling energy E_{tun} penetrating a 3D structured barrier. The critical difference between electron tunneling in proteins and conductivity in metals is that the electron does not form true intermediate states of the "bridge." That is, reduced bridge states do not persist for any detectable period of time. However, slight admixtures of the bridge states enter the effective donor and acceptor state (see Appendix A). It is this slight "contamination" of the donor and acceptor orbitals by the bridge orbitals that facilitates electron tunneling.

Tunneling energetics

Two types of virtual (i.e. energetically forbidden) intermediates facilitate tunneling. These involve forbidden species with extra electron(s) on the protein or electron(s) removed from the bridge (hole(s) injected) (Curry *et al*, 1995). The energy of a particular virtual intermediate is defined as the energy needed to oxidize or reduce the bridge (at the frozen geometry prior to electron removal or insertion). The energy of a given virtual intermediate defines the contribution of that intermediate to the tunneling process. This claim can be understood with the standard perturbation theory based argument of physical chemistry - states close in energy mix more strongly than those distant in energy. It is possible that electron and hole mediation propensity differ in distinct regions of a protein, are sensitive to side chain, structure and hydrogen bonding motif, are tunneling energy dependent etc. Bonding orbitals and lone pairs of electrons as well as antibonding orbitals of the protein are tunneling mediators. Because of the large energy gap between these

sets (defined by the binding energy and the electron affinity of the protein), the overall shape of the tunneling energy dependence forms a "smiley face;" coupling is strong for energies near the filled or empty states, but weaker and (weakly energy dependent) inbetween (see fig x). Details of these figures (the energy gap and asymmetry of the curves) depend upon the nature of the electronic structure model used. Considerable effort is now aimed at comparing the shape and asymmetry of these plots at different levels of electronic structure theory.

How does exponenetial decay arise from delocalized bridge states?

Much of physical organic chemistry is based upon orbital symmetry arguments and much of ET theory can be summarized with a few orbital interaction concepts (e.g., Fleming, 1976). However, in stark contrast to many examples in physical organic chemistry, frontier orbital mixing arguments fail. For example, consider a localized donor interacting with the frontier orbital of an alkane bridge. The HOMO (or LUMO) of the bridge is completely delocalized, with approximately equal electron density on each CH_2 unit of the chain. Thus, if the chain has 10 repeat units, about 1/10 of the electron density is located on each CH_2 of the HOMO or LUMO. Frontier orbital analysis would mix one (or both) of these states with the donor, forming a molecular orbital $\Psi \simeq \phi_D + \gamma\phi_{HOMO}$. γ is expected to be small, but since ϕ_{HOMO} is delocalized, the donor electron would be predicted to leak equally onto all sites of the bridge. Clearly a simple square barrier approximation of the alkane would suggest exponential decay of amplitude away from the donor. What is wrong with this simple frontier orbital analysis?

What is missing in the frontier orbital analysis is the fact that the energies of the orbitals below the HOMO (the HOMO-1, HOMO-2, $\cdots$ orbitals) are all about as close in energy to the tunneling energy (E_{tun} - the energy of the donor and acceptor states in electron transfer active geometry that lies in the HOMO-LUMO gap of the bridge) as is the HOMO itself. Thus, all of these states mediate the coupling of the donor electron through the bridge. Neglecting even one of the bridge orbitals in calculating the donor propagation can lead to nonphysical results. The subtle cancellation of oscillatory bridge wave functions leads to (approximately) exponential decay of coupling with distance. The need to include *all* states to reproduce the decay as well as the difficulty of conducting quantum calculations on large many-body systems has favored simple models that build in the essential physics of the tunneling problem. The development of quantum chemical methods to calculate electronic coupling in modest to large chemical and biochemical systems is the goal of many current efforts.

Through bond and through space decay length scales

There are two qualitatively different types of electronic interactions in chemical systems: through-bond interactions and through-space interactions. In ET reactions, we need to understand how through-bond vs. through-space interactions influence tunneling mediation. The strength of bond mediated coupling depends upon how rapidly a localized donor localized state decays. What determines how rapidly this state decays? The distance scale is determined principally by the atomic orbital hybridization of the atoms constituting the bonds, the energies of these orbitals, and the tunneling energy. For example, the very simplest analysis of carbon-carbon bonds interacting in a polyethylene chain suggests that the decay should be proportional to the 2s - 2p ionization potential difference for carbon divided by the tunneling energy (Beratan and Hopfield, 1984). Here, the key ratio is one of bond-bond interaction strength in units of the tunneling energy. A typical coupling decay per bond is found to be 0.6 in the experiments of Closs and Miller, for example (Closs and Miller, 1986). In contrast, the through-space distance decay is determined solely by the tunneling energy. In the extreme through-space limit (in 1D) this decay scales exponentially with a decay factor proportional to the square root of the tunneling energy. Through space decay of R Å is approximately $0.6\exp[(-1.7)(R-1.4)]$ for a 10 eV binding (tunneling) energy electron (Onuchic and Beratan, 1990). This expression interpolates between the decay per bond parameters (known from experiments) and the 1D decay expression for vacuum tunneling.

2.2 Tunneling pathways in proteins. Proteins consist of a sequence of peptide backbone interactions augmented by nonbonded interactions arising upon protein folding. In an attempt to mesh the relatively well understood through bond decay process with "short cuts" to tunneling provided by hydrogen bonds and van der Waals contacts in the folded structure, we built the Pathway model to estimate T_{DA}.

We have already presented enough information to estimate the strength of long range interactions in proteins! Since electron tunneling involves a combination of through bond and through space coupling, we need to assemble a combination of the two types of decay factors. Thinking of these through bond and through space factors as highly renormalized or rescaled parameters (more on this later) we write (Beratan *et al*, 1987; Onuchic and Beratan,1990; Beratan *et al*, 1992)

$$T_{DA} = A \prod_i \epsilon_C(i) \prod_j \epsilon_H(j) \prod_k \epsilon_S(k) \qquad (2.4)$$

Here A is a prefactor, and each ϵ is a decay per unit, described by the experiments or

simple estimates above. The hydrogen bonds can be analyzed as a whole (as was done originally) or broken into a combination of through-bond and through-space steps (as was done later) (Onuchic and Beratan, 1990; Beratan *et al* 1990; Regan *et al* 1993). The prefactor reflects the strength of the interaction between the charge localization sites and the bridge, as well as the relative energetics of the donor, bridge and acceptor orbitals (Regan *et al*, 1993).

Within the pathway strategy, any protein structure (from x-ray or NMR experiments) defines a network of pathway decay parameters. That is, every pair of atoms is connected through a covalent bond, a hydrogen bond, or through space. A list of simple decay factors corresponding to each connection type can be written using the simple parameterization above. Simple analysis gives:

$$\epsilon_C = 0.6 \tag{2.5a}$$

$$\epsilon_H = 0.6^2 e^{-1.7(R-2.8)} \tag{2.5b}$$

$$\epsilon_S = \frac{1}{2} 0.6 e^{-1.7(R-1.4)} \tag{2.5c}$$

The hydrogen bond decay is from heteroatom to heteroatom. The factor of 1/2 in the through-space factor is associated with orbital angular overlap effects. Within this prescription, estimating the coupling is simply a matter of listing the through bond or through space decay for every pair of atoms in the protein and then finding the combination of these interactions, beginning at the donor and ending at the acceptor, that maximizes the product of these penalty factors. This problem is no longer one of electron structure theory; it is one of graph theory (Betts *et al*, 1992). We have used numerous graph theoretical search strategies (breadth-first and depth-first searches, for example) to find the very strongest path or families of pathways in proteins. This computation is rapid even in very large proteins; software exists to perform these searches on workstations and personal computers.

What is the physical meaning of the dominant pathway?

The pathway decay parameters are taken from experiments and from simple theoretical estimates (Beratan *et al*, 1991). The estimated pathway coupling between donor and acceptor is the simple product $\epsilon_1 \epsilon_2 \cdots \epsilon_N$. And the "physical pathway" is comprised of the atoms associated with each of these decay factors. Yet, the physical pathway is an "effective" object because the decay parameters take into account the surrounding bonded and nonbonded interactions in an average sense. Since our through-bond decay factors

are estimated from experiment, and the experimental couplings incorporate bonded and non-bonded interactions to infinite order, the dominant physical pathway is really at the center of a set of physical pathways that enter the electronic coupling. We are currently developing new methods to dissect the contributions of the strongest physical pathway and surrounding paths to the electronic coupling. This analysis has led to the idea of fattened pathways (Regan *et al*, 1993), pathway tubes (Regan *et al*, 1995), contact importance factors (Skourtis *et al*, 1994), and pathway interference effects (Skourtis *et al*, 1995). It is important to realize that snipping one contact on the strongest pathway will not shut down electron transfer in general. Pathways arise in families, and *the strongest pathway is characteristic of those paths that dominate the electronic coupling*. Recent studies of fattened pathways and pathway tubes have shown more precisely what the shape of the relevant region surrounding the best path is in a given protein. To move beyond the simple pathway estimate of the coupling all possible sequences for the propagation of wave function amplitude between atomic orbitals of the bridge that begin with an orbital coupled to the donor and end with one coupled to the acceptor must be added together. Such summations can be computed using perturbation theory or Dyson expansion strategies, or by using techniques that explicitly sum all bridge pathways to infinite order (Onuchic *et al*, 1991; Goldman 1991; Ratner 1990; Regan *et al*, 1993; Gruschus and Kuki, 1993).

When does a simple product approximate the tunneling matrix element?

The product expression for T_{DA} looks like a perturbation theory (McConnell, 1961) result, but it is not. Product forms for electronic coupling are in fact much more general. For example (da Gama, 1990), any linear chain of orbitals with nearest neighbor coupling interactions can be shown to mediate electronic coupling in a manner that the coupling apperars as a product. Linear chains of orbitals with dangling side chains also yield a product expression for T_{DA} (eq 2.6).

$$T_{DA} \propto \prod_{i=1}^{N-1} \frac{\beta_{i,i+1}}{E_{tun} - \alpha_i - \Delta_i} \tag{4}$$

In this equation, α_i is a site energy and Δ_i is a site energy shift that arises from all possible "scattering pathways" of electron amplitude throughout both the main chain and the dangling side chains (daGama, 1990). E_{tun} is the tunneling energy and $\beta_{i,i+1}$ is the interaction between the (i) and (i+1) bridge units. In the extreme perturbation theory limit, a product expression ban be recovered. Once loops appear (provided by bonded or

non-bonded interactions) in the bridging structure, a simple product expression need no longer be valid. Complications may arise when simple hamiltonians are built neglecting dangling side chains, loops, etc. and the complicating aspects can be reintroduced and their role probed. The results, as one might expect, are protein structure dependent (Regan, *et al*, 1995).

Key role of H-bonds predicted

From model compound ET data, we know that proteins would be unable to transfer electrons if the electrons were able only to propagate down the covalent peptide backbone. The reason for this is that points close in distance are often far apart in amino acid sequence. As such, any realistic model of protein electronic interactions confronts the issue of what creates viable "short-cuts" for electron propagation. We proposed hydrogen bonds as tunnels for the electrons on the grounds of simple energy and overlap analysis. The hydrogen bond, in this framework, can be thought of as an interaction that creates very short through-space gaps between otherwise unconnected segments of the protein. Since the electron must propagate at least a small distance through-space to avoid a circuitous purely peptide backbone path, the ubiquitous hydrogen bond would seem to provide copious shortcuts. Since the average electron lone pair to hydrogen atom distance in a hydrogen bond is typically much smaller than van der Waals contact distances between other non-bonded atoms, we predicted a very special mediating role hydrogen bonds.

The key role for hydrogen bond contacts in ET proteins was first demonstrated by Therien and Gray in ruthenium modified systems (Therien *et al, 1991*). By fixing an ET probe at a specific surface site with a well defined protein medium inbetween, the predictions of the pathway model could be compared directly to experiments. Agreement was excellent. It was, perhaps, surprising that decay of coupling across a hydrogen bond was predicted to be about the same as that across two covalent bonds. This prediction itself was confirmed by small molecule experiments in the groups of Sessler (Harriman *et al*, 1992), Nocera (Turró *et al*, 1992), and Therien (de Rege *et*, 1995). This feature of hydrogen bonds is remarkable, and further studies of the energetic, structural, and dynamical aspects of the hydrogen bond in the context of electron transfer is needed.

2.3 Predictions of the tunneling pathway model.

What are the key predictions of the tunneling pathway model? They are basically five-fold (Beratan *et al*, 1991, 1992).

Coupling can be approximated as a product of decay factors characteristic of the

chemistry of the medium intervening between donor and acceptor.

A key role of covalent and hydrogen bonds as tunneling mediators and a less important role for van der Waals interactions is anticipated.

The average scale of coupling decay with distance arises from the balance of through-bond and through-space decay. Coupling down a straight chain (as in a β-strand is expected to be about the same as that found in simple model compounds with similar donor-acceptor energetics. In systems with somewhat more circuitous tunneling routes (i.e., most ET systems), the decay of coupling with distance is expected to be somewhate faster and to depend upon the secondary and tertiary structure of the folded protein.

Decay of coupling throughout proteins is anisotropic. Coupling is expected to drop with distance, but considerable scatter about a single exponential line is anticipated. This anisotropy gives rise to hot and cold spots for electron transfer. Subsets of coupled sites within a given protein can always be found that fall on a single exponential line.

The average distance decay is tied to protein secondary structure.

All of these predictions have been scrutinized in the context of ruthenium modified proteins (Winkler and Gray, 1992; Onuchic *et al*, 1992) and the photosynthetic reaction center (Curry, 1995).

Tests of pathway predictions

The essential role of hydrogen bonding in protein ET was demonstrated by Gray (Therien *et al*, 1991; Onuchic *et al* 1992). The anisotropy of rates in proteins was shown in numerous Ru cytochrome *c* experiments. Derivatives with distances differing by up to 7 Å were shown to have the same rate. Other derivatives with essentially the same distance were shown to have rates differing by 3 or 4 orders of magnitude. Through backbone coupling cannot account for these rates at all, nor can a model that assumes that purely through-space contacts control ET. If the through space contacts dominated, much of the structure dependence of the rates would simply be washed out.

Just as early experiments showed the importance of hydrogen bonding, later experiments confirmed the cost associated with through space contacts. The Ru(His 72) cytochrome *c* data point is critical in this regard. In this derivative, the transfer distance is only 8.4Å (edge-to-edge) but the maximal (computed for an activationless process) is a surprisingly slow 9×10^5 sec^{-1} (Wuttke *et al* 1992). The pathway analysis clearly shows a through space gap along the dominant donor acceptor pathway (or pathway family). Other modified protein systems show rate anomalies or secondary structure dependencies that can only be understood in the context of pathway analysis (Therien *et al* 1991;

Wuttke *et al* 1992; Langen *et al*, 1995; Karpishin *et al*, 1994; Moreira *et al*, 1994).

Pathways in the exponential distance regime

Much of our discussion has emphasized the possible nonexponential decay of coupling that can arise in a protein. However, subsets of couplings in a given protein may be *highly* exponential. For example, we predicted that coupling down the β-strand of azurin would be just such a case (Beratan *et al*, 1992). This prediction was recently confirmed in a family of Ru-azurin experiments (Langen *et al*, 1995, Regan *et al*, 1995). These subsets of data associated with a single strand are essentially exponential, despite the fact that scatter of coupling with distance in azurin is predicted, over the entire protein, to be as large as in cytochrome *c*.

Dutton has pointed out that the rates of ET in the photosynthetic reaction center (Gunner, 1991), when corrected for activation energy differences, fall on an exponential distance line (Moser *et al*, 1992). This correlation is entirely consistent with pathway analysis as well (Curry *et al*,1995) and arises from relatively direct pathways between the chromophores. Thus, one must realize that subsets of data may be exponential or nonexponential with distance, depending upon how the pathway coupling within that family scales with distance.

Docking and intermolecular ET

An important step in biological ET is often *inter*molecular (see Stemp and Hoffman, 1993 and Pelletier ahd Kraut, 1992 for examples). Much theoretical work on protein ET has been confined to *intra*molecular reactions. The pathway model was recently extended to describe *inter*molecular ET by combining the pathway couplings in each individual protein with an additional interface (through-space or hydrogen bond) decay factor using eq 2.5 (Aquino *et al*,1995):

$$T_{DA} \propto \Pi_i \epsilon_{\rm D}(i) \Pi_j \epsilon_{\rm A}(j) \epsilon_{\rm inter} \qquad (2.7)$$

Here, $\Pi_i \epsilon_{\rm D}(i)$ is the electronic coupling decay between the electron donor site and the surface of the protein containing the electron donor; $\Pi_j \epsilon_{\rm A}(j)$ is the electronic coupling decay between the electron acceptor site and the surface of the protein containing the acceptor; and $\epsilon_{\rm inter}$ is the electronic coupling decay between protein surfaces (i.e., a through-space or hydrogen bond coupling between surface atoms on the two proteins). Note that in eq. 4, $\epsilon_D(i)$ and $\epsilon_A(j)$ can be any of the three types of decay (i.e., covalent, hydrogen-bonding, or through-space). This factored electronic coupling separates quantities that are well-defined, $\Pi_i \epsilon_{\rm D}(i)$ and $\Pi_j \epsilon_{\rm A}(j)$, from a quantity that is less well defined, $\epsilon_{\rm inter}$.

Surface to redox center couplings are obtained for each protein in the usual way; maps of these couplings identify regions of the protein that efficiently couple electron transfer between the redox site. Matching the strongly coupled regions will result in the maximal intermolecular electron transfer (if ϵ_{inter} is not too small) and can be used as a criterion to evaluate possible docked structures. This criterion will supplement other energetic constraints on possible structures of functional importance in bimolecular ET.

Concerns related to simple pathway analysis.

A number of basic questions enter the analysis of when pathway methods break down. The obvious chemical issue is how appropriate it is to approximate all atoms types and bonds as being the same. This approximation sounds disasterous, but is justified by the fact that the tunneling energy is several eV removed from the energies of the mediating bonds, and a distribution of bond types appear in pathways. As such, small energy differences might be less important that in other kinds of chemical reactions and a certain amount of averaging may take place.

A large number of physical (and an even larger number of scattering) paths exist between donor and acceptor. How significant is the role played by quantum interference between pathways? The answer to this question should depend upon seconday and tertiary structure. In cytochrome c, we showed that couplings to ruthenation sites could be well approximated by adding to the best pathway the chemical bonds dangling from the path and including including in all scattering contributions arising from these groups. Within this set of orbitals, the coupling can be calculated in a way that includes all pathway interferences (to infinite order) and the final result is nearly identical to that found in when the entire protein is included in the calculation. The case of azurin, where donor and acceptor sites are separated by many β−strands, is more complicated.

In proteins, a number of other complications is clearly present and is receiving current attention. For example, fluctuations in atom-atom distances must lead to averaging of pathway couplings, especially the through space couplings. This may be yet another reason that a simple parameter set works so well. Much of biological ET involves bimolecular processes. We are just beginning to probe the balance between docking energetics and pathway matching, and this may be another case were intra- and inter-protein fluctuations are critical. Finally, the donor and acceptor electronic structure plays an essential role in the ET process. Efforts are underway to splice improved local electronic structure results together with pathway or pathway-like calculations (Kurnikov and Beratan, 1995). The deepest conceptual concern about the pathway approach is the

neglect of coupling between interacting pathways.

2.4 Beyond the single pathway view.

What is the physical meaning of a tunneling pathway?

As was discussed in section 2.3, a tunneling pathway lies at the core of a protein region that mediates the donor-acceptor interaction. The pathway model is parameterized such that it builds in the effect of surrounding mediating residues because parameters were extracted from chemical model systems with multiple paths. As such, one should not expect, necessarily, that breaking a contact in the best path will shut down (or even noticibly influence!) the rate of electron transfer. It should be easier to strengthen a weak pathway by making protein mutations than to weaken a family of strong pathways. Thus, the best pathway is characteristic of the cluster of paths that provides donor-acceptor coupling. To quantify the role of other paths, approaches that build an explict hamiltonian for the electronic interactions in the protein are necessary. Thus, the challenge is to build such a hamiltonian and then to interpret it in the language of pathways.

Multi-path models and electron/hole propagators.

How can the average multi-path effects in the pathway analysis be made more explicit? The donor-acceptor interaction mediated by a multi-orbital bridge can in fact be described in a concise manner that includes multiple pathways and interference between pathways. Imagine solving the electronic structure problem for the isolated bridge. In the linear combination of atomic orbitals-molecular orbital (LCAO-MO) approximation, this calculation would produce a set of MOs for the bridge:

$$\Psi^{(i)}_{protein} = \sum_{j=1}^{M} c_j^{(i)} o_j \tag{2.8}$$

where: j - AO index; i - MO index

For simplicity, we assume that the donor interacts only with site number 1 of the bridge (with interaction energy V_{D1}) and that the acceptor interacts only with site number N of the bridge (with interaction energy V_{NA}). This is a special case of eq 7 in the appendix. Then the donor-acceptor interaction mediated by the bridge is:

$$T_{DA} = V_{D1}\left[\sum_i \frac{c_1^{(i)} c_N^{(i)}}{E_{tun} - E^{(i)}}\right] V_{NA} \tag{2.7}$$

Here $E^{(i)}$ is the energy of the i^{th} MO of the protein (Larsson, 1981).

This expression accounts for all physical and scattering pathways to infinite order within the protein. The donor-protein and acceptor-protein interactions enter to first order. Protein MO's are weighted in eq 2.7 based on their proximity to the tunneling energy (denominator of equation) as well as their degree of localization near the donor (the AO coefficents appearing in the numerator). The coefficients and their products in the numerator are expected to be oscillatory in magnitude and sign for a given MO. However, *the sum* of coefficient products divided by the energy terms decays with the physical distance between sites 1 and N.

The pathways strategy provides a means of approximating the tunneling matrix element T_{DA}. The ability of a bridge to propagate single or multiple electrons and/or holes is contained in the Green's function, G, which is closely related to eq 2.7. The Green's function includes the energetic and orbital effects describe above and all bridge pathway effects. In the molecular orbital language, the green's function matrix element G_{1N} is the quantity in the square brackets of eq 2.7. In this simple case, G_{1N} multiplied by D and A interactions is equal to T_{DA}. In cases where D and A interact with more than one bridge orbital, a sum over the interacting sites must be performed to calculate T_{DA}.

Hamiltonian based models of electronic coupling in proteins.

The critical featured in coupling calculation are balancing through-bond vs. through space interactions and choosing appropriate values for the tunneling energy.

Pathway-based strategies.

An average decay per bond of ϵ in a linear chain molecule can be associated with a few molecular parameters. For example, if the chain is approximated as consisting of one orbital per bond (say a C-C sigma bond), dangling bonds (perhaps CH bonds) are neglected, and overlap is ignored, the relation between ϵ, the inter-bond coupling (γ) and the tunneling energy is simply

$$\epsilon + 1/\epsilon = E_{tun}/\gamma \qquad (2.10)$$

Note that this equation (valid in the long chain limit) includes all high-order (scattering) pathways. As such, given a value for the per bond decay constant, a hamiltonian based method can be parameterized (for a given tunneling energy). Recently, this kind of model was used to analyze electronic propagation in azurin (Regan et al, 1995). In these caluclations, hamiltonian elements (γ) provide interactions between neighboring chemical bonds that share a common atom. Hydrogen bonds were treated as two interacting covalent bonds, and through space interactions were set to zero.

Other strategies.

Other approaches have used standard Hamiltonians from the literature or have built custom ones for electron and/or hole mediated superexchange. The earliest work in this direction assumed an electron mediated superexchange mechanism to construct an effective hamiltonian; the coupling element was calculated with a path integral strategy (Kuki and Wolynes, 1987).

Most other calculations have utilized Green function strategies (see sect. 2.4 above) and a molecular orbital approach. Custom hamiltonians aimed at treating hole mediated superexchange (Gruschus and Kuki, 1993) and standard hamiltonians that include both electron and hole superexchange have been utilized. Some of these strategies first determine important protein regions with a pathway search and then compute coupling on a fragment of the protein with a Green function method built upon a simple electronic structure model. These methods are often carried out at the extended Hückel level (see Siddarth and Marcus, 1993, for example). These calculations can be tested for size dependence to determine whether or not all relevent amino acids have been included. Some of the fragment approaches use self-consistent field methods, which generate electronic densities of states for the proteins that are more meaningful than those of one-electron methods (see Curry et al, 1995 for discussion of this important point).

Extended-Hückel calculations on proteins the size of cytochrome *c* are now routinely accessible (Regan *et al*, 1993), and self-consistent field (SCF) methods should be approachable in the near future. SCF calculations will provide an importante advance, as the extended- Huckel calculations are known to misrepresent the nature of the virtual oxidized and virtual reduced mediating states. It is fairly clear, too, that new methods for digesting the vast array of information generated in these large- scale electronic structure calculations is needed.

As more advanced methods are developed, the simplicity and obvious ease of interpretation associated with pathway analysis is lost. Hybrid strategies that compute interactions using Green's function methods (adding up high-order interfering pathways) beginning with a simple pathway, fattened pathways, or pathway tube provide a helpful, perhaps essential, context in which to understand electronic propagation in proteins. For example, analysis of this kind can show whether trivial interferences (arising from bonds dangling off the dominant path but not participating in paths themselves) or qualitatively distinct multiple pathway effects influence coupling in a particular protein structure. Analysis of this kind can also explain why or why not electronic propagation in specific

proteins is anisotropic.

2.5 Current challenges.

There are at least three aspects of bridge mediated electronic interactions that theoretical methods are yet to come to terms with. The first is the combined electron and hole mediation of tunneling. That is, models must be built in such a way that virtual motion of excess electrons as well as excess holes is accounted for in proper balance. Hole mediation is expected to be of particular significance in thermal ET processes, while electron mediation should be of greater importance in photoinduced ET (although hole mediation can dominate even in this regime as well). The mediation of tunneling across hydrogen bonds is anticipated to have a significant hole component arising from the electron lone pair. The second critical aspect of the bridge treatment is that the theoretical methods must build in the proper qualitative energetics of the bridge virtual states. That is, methods must reproduce the energetics of virtual cation or anion states of the bridge. One electron methods (with standard parameterizations) reproduce the N-electron properties of the bridge qualitatively, but cannot simultaneously incorporate both the electron and hole energetics using standard parameterizations (Larsson, 1988 proposed a parameterization to avoid this problem). Finally, a challenge for Hamiltonian or Green's function methods is to construct the proper through-space decay of the electronic states. Basis functions commonly used in quantum chemistry are built from atomic orbitals. The decay of atomic orbital wavefunctions is set by atomic binding energies. Far from the nuclei (i.e., in through space contacts), molecular orbitals must decay with an exponent determined by the molecular orbital binding energy, not the energies of the constituent atoms. It is not yet clear if standard basis set strategies will adequately reproduce through-space decay in the intermediate distance regime associated with van der Waals contacts (3-4 Å).

Whether derived from first principles or not, ET analysis requires a better understanding of through-space and hydrogen bond mediated couplings. These interactions are surely orientation and energy dependent, yet we have limited information from model systems or theory. Of particular importance is the role of fluctuation in the through-space contacts and the possibilty of dynamically averaging these couplings and their decay factors.

Electronic structure methods based upon independent-electron models (those upon pathway decay parameters or the extended-Hückel hamiltonian) can be parameterized through the tunneling energy to give reasonable estimates of coupling for closely re-

lated families of reactions. However, in these simple hamiltonians the bridge energetics lacks qualitative agreement with experiment. As such, these methods are not expected to display the proper overall tunneling energy dependence. Methods that reproduce experimental ionization potentials and electron affinities of the bridge (rather than optical gaps) are anticipated to give more reliable estimates of protein mediated coupling. Large scale self-consistent field calculations are expected, therefore, to play an increasing role in ET coupling analysis.

A current related challenge in biomolecular ET is to understand the recent reports of ET in DNA (Meade and Kayam, 1995; Murphy *et al*, 1993; Brun and Harriman, 1992). One particular system shows quenching, assumed to arise from electron transfer over extremely long range. Recent theoretical analysis that generates an appropriate energy scale, predicts average distance decays with distance as large or larger than was found in proteins (Priyadarshy *et al*, 1995). This can be understood in the context of tunneling pathways involving 3.4 Å through-space contacts between base pairs or by analyzing the through bond pathways along the ribose phosphate backbone. Because the electron affinity and ionization potentials of DNA are similar to proteins (compared to a tunneling energy of about -5 eV), the average distance dependences are predicted to be about the same.

Pathway analysis shows some simple expectations related to secondary structure and tertiary protein motif. For example, decay with distance is expected to be less rapid when donor and acceptor are connected with a β-strand of protein. Propagation down an α-helix is somewhat weaker, and coupling orthogonal to helicies, is predicted to be even more rapidly decaying. This analysis is based upon simple connectivity arguments, and has been confirmed by experiment. A current challenge is to understand whether pathway interference in various secondary structures and tertiary motifs causes substantial deviations from the more basic pathway analysis. This should be a rich area for creative use of theory and experiment in the future.

Acknowledgments

We are grateful to our collaborators for discussion of these ideas with us. This work is supported by the National Science Foundation (CHE-9257093 and MCB-9316186), the National Institutes of Health (GM48043-2), and the Department of Energy (DE-FG36-94G010051).

REFERENCES

Aquino AJA, Beroza P, Beratan DN, Onuchic JN. (1995) Docking and electron transfer between cytochrome c_2 and the photosynthetic reaction center. Chem. Phys., 197: 277-288

Bard AJ and Faulkner LR (1980) *Electrochemical methods*, Wiley, New York.

Beratan DN and Hopfield JJ (1984) Calculation of electron tunneling matrix elements in rigid systems: mixed valence dithiaspirocyclobutane molecules. J Am Chem Soc 106: 1584-1594.

Beratan DN, Onuchic JN, Hopfield JJ. (1987) Electron tunneling through covalent and noncovalent pathways in proteins. J. Chem. Phys. 86: 4488-4498.

Beratan DN, Onuchic JN, Betts JN, Bowler BE, Gray, HB (1990) Electron tunneling pathways in ruthenated proteins. J Am Chem Soc 112: 7915-7921.

Beratan DN, Betts, JN, Onuchic, JN (1991) Protein electron transfer rates set by the bridging secondary and tertiary structure. Science 252: 1285-1288.

Beratan DN, Onuchic, JN, Winkler, JR, Gray, HB (1992) Electron tunneling pathways in proteins. Science 258: 1740-1741.

Beratan DN, Betts JN, Onuchic, JN (1992) Tunneling pathway and redox state dependent electronic couplings at nearly fixed distance in electron transfer proteins. J Phys Chem 96: 2852-2855.

Bertini I, Gray HB, Lippard S, Valentine, J (1994). *Bioinorganic Chemistry*, University Science Books, Mill Valley, CA

Betts JN, Beratan DN, Onuchic JN (1992) Mapping electron tunneling pathways: an algorithm that finds the "minimum length"/maximum coupling pathway between electron donors and acceptors in proteins. J Am Chem Soc 114: 4043-4046.

Brun AJ and Harriman A (1992) Dynamics of electron transfer between intercalated polycyclic molecules - effect of interspersed bases. J. Am. Chem. Soc. 114: 3656-3660.

Calef DF and Wolynes PG (1983) ?Title? J. Phys. Chem. 87: 3387-3400.

Closs G and Miller JR (1986) Distance, stereoelectronic effects, and the Marcus inverted region in intramolecular electron transfer in organic radical anions. J Phys Chem 90: 3673-3683.

Curry WB, et al. (1995) Pathways, pathway tubes, pathway docking, and propagators in electron transfer proteins. J. Bioenerg. Biomembranes 27: 285-293.

daGama AAS (1990) Through bond electron transfer interaction in proteins. J Theor Biol 142: 251-260.

deRege PJF, Williams SA, Therien MJ (1995) Direct evaluation of electronic coupling mediated by hydrogen bonds: implications for biological electron transfer. Science 269:1409-1413.

DeVault D (1984) *Quatum mechanical tunneling in biological systems, 2nd ed.* Cambridge Press, New York.

Fleming, I. (1976) *Frontier orbitals and organic chemical reactions* Wiley, New York.

Garg A., Onuchic JN, Ambogoakar V (1983) Effect of friction on electron transfer in biomolecules. J. Chem. Phys. 83: 4491-4503.

Goldman C (1991) Long range electron transfer in proteins - a renormalized perturbation expansion approach. Phys Rev A, 43: 4500-4509.

Gruschus JM and Kuki A (1993) New hamiltonian model for long range electronic superexchange in comples molecular structures. J Phys Chem 97: 5581-5593.

Gunner M (1991). Curr Topics Bioenerg 16: 319-367.

Harriman A, Kubo Y, Sessler JL (1992), ?Title? J Am Chem Soc 114: 388-???.

Hopfield JJ (1974) ?Title?. Proc Natl Acad Sci (USA). 71: 3640-3644.

Karpishin TB, Grinstaff M, Komar-Panicucci S, McLendon G, Gray HB (1994) Electron transfer in cytochrome c depends upon the structure of the intervening medium. Structure 2: 415-422.

Kuki A and Wolynes PG (1987) ?Title?. Science 236:1647-16??.

Kurnikov IV and Beratan DN (1995) A fragment approach to electron transfer in macromolecules. In preparation.

Langen R, Chang IJ, Germanas JP, Richards JH, Winkler JR, Gray HB (1995) Electron tunneling in proteins: coupling througha a β strand. Science 268: 1733-1735.

Larsson S (1981) ?Title?. J Am Chem Soc 103: 4034-4040.

Larsson S, Broo A, Kallebring B, Volosov A (1988) Long distance electron transfer. I J Quantum Chem: Quantum Bio Symp 15: 1-22.

Lippard SJ, Berg JM (1994). *Principles of Bioinorganic Chemistry*, University Science Books, Mill Valley, CA.

Meade TJ and Kayyem JF (1995) Electron transfer through DNA - site specific modification of duplex DNA with ruthenium donors and acceptors Angew. Chem. Int. Ed. Engl. 34:352-354.

Murphy CJ, Arkin MR, Jenkins Y, Ghatlia ND, Bossmann SH, Turro NJ, Barton JK (1993) Long range photoinduced electron transfer through a DNA helix. Science 262: 1025-1029.

McConnell H (1961) ?Title?. J Chem Phys 35:508-515.

Moser CC, Keske JM, Warncke K, Farid RS, Dutton PL (1992) Nature of biological electron transfer. Nature 355: 796-802.

Moreira I, Sun J, Cho M, Wishart J, Isied S (1994) Electron transfer from the heme of cytochrome c to two equidistant redox modified sites, histidine 33 and methionine 65 - the importance of electronic effects and peptide networks. J Am Chem Soc 116: 8396-8397.

Onuchic JN, deAndrade PCP, Beratan DN (1991) Electron tunneling pathways in proteins - a method to compute tunneling matrix elements in very large systems. J Chem Phys 95: 1131-1138.

Onuchic JN, Beratan DN, Winkler JR, Gray HB (1992) Pathway analysis of protein electron transfer reactions. Ann Revs Biophys Biomol Struct 21: 349-377.

Onuchic JN and Beratan DN (1990) A predictive theoretical model for electron tunneling pathways in proteins. J Chem Phys 92: 722-733.

Onuchic JN, Beratan DN, Hopfield, JJ (1986) Some aspects of electron transfer reaction dynamics. J Phys Chem 90: 3707-3721.

Onuchic JN, and Wolynes, PG (1988) J. Phys. Chem. 92: 6495-????.

Pelletier H and Kraut J (1992) Crystal structure of a complex between electron transfer partners, cytochrome c peroxidase and cytochrome c. Science 258: 1748-1755.

Priyadarshy S, Risser SM, Beratan DN (1995) Electron transfer in DNA: tunneling orthogonal to a π-way. In preparation.

Ratner MA (1990) Bridge assisted electron transfer - effective electronic coupling. J Phys Chem 94: 4877-4883.

Regan JJ, Risser SM, Beratan DN, Onuchic JN (1993) Protein electron transport: single versus multiple pathways. J Phys Chem 97: 13083-13088.

Regan JJ, DiBilio AJ, Langen R, Skov LK, Winkler JR, Gray HB Onuchic JN Chemistry and Biology (1995) Electron tunneling in azurin: the coupling across a β-sheet. 2: 489-496.

Siddarth P and Marcus RA (1993) Correlation between theory and experiment in electron transfer reactions in proteins - electronic couplings in modified cytochrome c and myoglobin derivatives. J Phys Chem 97: 13078-13082.

Skourtis SS, Regan JJ, Onuchic JN (1994). Electron transfer in proteins - a novel approach for the description of donor acceptor coupling. J Phys Chem 98: 3379-3388.

Skourtis SS, Beratan DN, Onuchic JN (1995). A method to analyze multi-pathway effects on protein mediated donor acceptor coupling interactions. Inorg Chim Acta, submitted.

Stemp EDA and Hoffman BM (1993) Cytochrome c peroxidase binds 2 molecules of cytochrome c - evidence for a low affinity, electron transfer active site on cytochrome c peroxidase. Biochemistry 32: 10848-10865.

Sutin N and Marcus RA (1985) ?Title?. Biochim Biophys Acta 811: 265-322.

Therien MJ, Bowler BE, Selman MA, Gray HB, Chang IJ, Winkler JR (1991) Long range electron transfer in heme proteins: porphyrin-ruthenium electronic couplings in three Ru(His)cytochromes c. In *Electron transfer in inorganic, organic and biological systems, Advances in Chemistry Series 228* ACS Press, Washington, DC, pp 191-199.

Turró C, Chang CK, Leroi GE, Cukier RI, Nocera DG Y ?Title? J Am Chem Soc 114: 4013-???.

Winkler JR and Gray HB (1992) ?Title?. Chem. Rev. 92: 369-379.

Wuttke DS, Bjerrum MJ, Winkler JR, Gray, HB (1992) Electron tunneling paths in cytochrome *c*. Science 256: 1007-1009.

Zusman LD (1994) Dynamical solvent effects in electron transfer reactions. Z Phys Chem 186: 1-29.

9/26/95

Appendix A: Electron transfer rate calculations

José Nelson Onuchic[1] and David N. Beratan[2]

[1] *Department of Physics, University of California, San Diego, La Jolla, CA 92093*

[2] *Department of Chemistry, University of Pittsburgh, Pittsburgh, PA 15260*

The goal of this appendix is to provide the reader with a connection between the common expressions for electron transfer rates and some of the deeper theoretical underpinnings. We hope to present a somewhat unified view of the popular rate expressions that are valid in limiting cases. We take this strategy because a number of excellent conventional approaches for deriving the rate expressions exit (Newton and Sutin, 1984; Marcus and Sutin, 1985; Mikkelsen and Ratner, 1987; Ulstrup, 1979; Devault, 1984; Onuchic *et al*, 1986; Jortner,1980), but a unified view utilizing modern perspectives and notation seems needed.

We will introduce the basic concepts associated with the calculation of unimolecular electron transfer (ET) rates. Special attention is given to non-adiabatic ET, since this is the limit most relevant to long-distance biological ET processes. In ET reactions, an electronic state is "created" in some spatial region (by a prior ET reaction, photoexcitation,

etc.), and one wants to calculate the rate at which this electron transfers to a different site localized elsewhere in space. Following creation of the initial state, the ET reaction is generally a radiationless process (although in some cases electron-hole recombination is associated with luminescence). The task before us is how to describes this ET event.

A.1 The ET Hamiltonian

Clearly, we need to define two electronic states, the donor (D) and acceptor (A) localized states. Our goal is to show how to obtain the effective hamiltonian that has been used extensively to study the generic ET problem (Garg *et al*, 1985; Onuchic, 1987; Wolynes, 1987; Onuchic *et al*, 1992; Skourtis and Onuchic, 1993):

$$H_{ET} = T_{DA}(\vec{Q})\sigma_x + \frac{1}{2}\left(\alpha_D^{eff}(\vec{Q}) + \alpha_A^{eff}(\vec{Q})\right) + \frac{1}{2}\left(\alpha_D^{eff}(\vec{Q}) - \alpha_A^{eff}(\vec{Q})\right)\sigma_z + H_Q. \quad (1)$$

T_{DA} is the tunneling matrix element between donor and acceptor. σ_x and σ_z are the Pauli matrices. "Spin-states" of +1 or -1 correspond to donor or acceptor localized states respectively. respectively. We are not dealing with an actual spin flip, but rather with another two-state (D and A) system. The spin-up/spin-down language is borrowed simply so that we can utilize a standard notation.

$$< up|\sigma_z|up >= 1 \quad , < down|\sigma_z|down >= -1 \quad \text{and} \quad < up|\sigma_z|down >= 0$$

and

$$< up|\sigma_x|up >= 0 \quad , < down|\sigma_x|down >= 0 \quad \text{and} \quad < up|\sigma_x|down >= 1$$

Terms that appear in brackets, $|>$ and $<|$, represent spin wave functions and the complex conjugate of a spin wave function respectively. The "up" state refers to the electron on D and the "down" state to the electron on A.

H_Q supplies the dynamics for the nuclear coordinates ($\vec{Q}$). $\alpha_D^{eff}(\vec{Q})$ ($\alpha_A^{eff}(\vec{Q})$) is the instantaneous (electronic) energy for the reactant (product) state. This equation assumes that the D and A electronic states are computed at frozen nuclear configurations, i.e. the Born-Oppenheimer approximation is assumed.

A.2 Two-level systems

For a given nuclear configuration, the strategy for constructing of the electronic part of the effective Hamiltonian is Löwdin partitioning (Löwdin, 1962). This approach was introduced to ET by Larsson (Larsson, 1981) and has been used extensively to investigate the effect of bridge structure on T_{DA}. There has been a significant effort aimed at computing T_{DA} in different ET systems; this is the topic of Chapter 2. As discussed there, the reduction of a many-orbital system to two-states requires that the tunneling energy of a transferring electron (E_{tun}) be specified. This tunneling energy reflects the binding energy of an electron associated with the donor in the geometry of the activated complex. This energy (and its relative value with respect to the orbital energies of the bridge), and the structure of the bridge determine the donor-acceptor coupling. E_{tun} appears as a parameter in the effective matrix element T_{DA}. In actual computations, E_{tun} is usually set equal to the average of the D and A energies and its value can be improved iteratively. Skourtis and coworkers have examined how to perform such a reduction for single- many-electron hamiltonians (Skourtis and Onuchic, 1993; Skourtis *et al*, 1993). They also described how to obtain the optimal value for E_{tun} and the limits of validity for this approach. As an example, we will show how this reduction is done for a general one-electron hamiltonian. The electronic hamiltonian can be written in matrix notation as:

$$\begin{pmatrix} H_{DA} & H_{DA,B} \\ H_{B,DA} & H_{Bridge} \end{pmatrix}, \tag{2}$$

where H_{DA} is the hamiltonian matrix that includes only the relevant donor and acceptor orbitals. The direct coupling between D and A in the case of long distance transfer is negligible. H_{Bridge} is the hamiltonian matrix for the bridge and $H_{B,DA}$ is the matrix that couples the donor and acceptor to the bridge. Löwdin diagonalization yields a reduced 2×2 matrix.

$$H_{DA} = H_{DA} - H_{DA,B} H_{Bridge}^{-1} H_{B,DA}. \tag{3}$$

This reduced matrix is:

$$\tilde{H}_{DA} = \begin{pmatrix} \alpha_D^{eff}(E) & T_{DA}(E) \\ T_{AD}(E) & \alpha_A^{eff}(E) \end{pmatrix}. \tag{4.a}$$

where

$$\alpha_{D(A)}^{eff}(E) = \alpha_{D(A)} + \Delta_{D(A)}(E). \tag{4.b}$$

$$\Delta_{D(A)} = \sum_{i,j} v_{D(A)i}\, G_{ij}(E)\, v_{jD(A)}, \tag{4.c}$$

and

$$T_{DA} = \sum_{i,j} v_{Di} G_{ij}(E) v_{jA}. \tag{4.d}$$

The i's and j's in the sums run over the bridge orbitals. G is the Green function for the bridge, i.e., the Green's function associated with H_{el} in the absence of the donor and acceptor. $G = (H_{Bridge} - E)^{-1}$.

E_{tun} and the Condon approximation

Eq. 4a is equivalent to eq. 3; the eigenvalues of the two equations are the same. Of the thousands of molecular orbitals present, we are only interested in two states that define the two-level system. The first step in analyzing the two states of interest is to compute the tunneling energy. The effective donor energy can be obtained from eq. 4 by solving

$$\alpha_D = \alpha_D^{eff}(\alpha_D). \tag{5}$$

The roots of this equation closest to α_D is the effective donor energy. A similar calculation can be performed for the acceptor. The tunneling energy, E_{tun}, is obtained for the nuclear configuration $\vec{Q}$ that brings donor and acceptor energies into coincidence:

$$E_T = \bar{\alpha}_D = \bar{\alpha}_A. \tag{6}$$

This configurational constraint is required because the process is radiationless, and is known as the Condon approximation. After calculating the tunneling energy, we finally extract the two-level system by fixing the value of E in eq. 4 equal to E_{tun}. How good is this approximation? It is reasonable for most of the ET problems discussed in this book, and limitations have been considered (Skourtis and Onuchic, 1993; Skourtis *et al*, 1993). Calculations of the matrix element T_{DA} given by eq. 4d is the focus of the Chapter 2. In most cases, (and this is assumed in the following discussion), ET occurs only when the donor and acceptor energy levels match, so T_{DA} is assumed constant with a value equal to the one obtained for the nuclear configuration in which these two energies are the same. Problems may arise for the Condon approximation when T_{DA} itself is strongly E_{tun} dependent.

The electronic coupling computed at an appropriate tunneling energy can be rewritten in a molecular orbital language as

$$T_{DA} = \sum_{n}^{(MO)} \sum_{i,j}^{(AO)} \frac{V_{Di} C_i^{(n)} C_j^{(n)} V_{Aj}}{E_{tun} - E^{(n)}}. \tag{7}$$

As noted in Chapter 2: (1) the summation involves an energy denominator, so as E_{tun} approaches the bridge states, coupling is enhanced. If E_{tun} falls below the bridge HOMO or above the bridge LUMO bridge localized intermediates can form and this is not the case of interest in most protein mediated ET reactions. (2) The bridge wave function coefficients $C_i^{(n)}$'s are oscillatory, and only upon summation of the product of coefficients does roughly exponential decay of coupling with distance emerge. (3) The nature of the bridge interaction with D and A enters through prefactors (V's) that are expected to be large near D and A, but small elsewhere.

Born-Oppenheimer approximation

The prior discussion is framed in the context of the Born-Oppenheimer separation of electronic and nuclear motion. For the Born–Oppenheimer approximation to hold, electronic energy separations must be large compared to relevant nuclear excitation energies. In addition, as the electron tunnels from the donor to the acceptor, it spends a "time" in the classically forbidden region (Beratan and Hopfield, 1984; Onuchic *et al*, 1986; Bialek *et al*, 1989). If this time is much shorter than the period of the vibrational motion coupled to ET, the tunneling electron sees nuclei at fixed positions, — that is, the Born–Oppenheimer approximation works. These approximations are reasonably good for electron transfer at moderate distances in proteins. In extremely long range ET, for example between quinone B of the photosynthetic reaction center and cytochrome c (Feher *et al*, 1989) or between D and A at random distances in a frozen glass (at long times) (Miller *et al*, 1989), the Born-Oppenheimer approximation itself is called into question.

A.3 Rate expressions

Now that the electronic part of the effective hamiltonian has been described, we turn to the nuclear coordinates ($\vec{Q}$) that cause the D and A electronic levels ($\alpha_D^{eff}(\vec{Q})$ and $\alpha_A^{eff}(\vec{Q})$ of eq 1) to fluctuate.

Simple models of vibronic (electron-nuclear) coupling lead to electronic energies that vary linearly with nuclear coordinate, $\vec{Q}$ (Onuchic *et al*, 1986). If the nuclear coordinate is a single harmonic (collective) coordinate and the donor and acceptor energies (α's) vary linearly with $\vec{Q}$, one can combine this linear term with the quadratic nuclear term by completing the square when writing the full nuclear potential energy and recover two parabolic nuclear potential energy surfaces, or "Marcus parabolas" for $\sigma_z = \pm 1$ (see figure A.1). The linear terms in the nuclear coordinate are different, depending upon whether the state is D^+A^- or DA^*. H_Q is harmonic with reorganization energy $\lambda = M\Omega^2(Q_D - Q_A)^2/2$ and ϵ is the driving force. $(Q_D - Q_A)$ represents the shift in

the equilibrium geometry upon ET.

An important part of eq. 1 not discussed so far represents the remaining nuclear degrees of freedom in H_Q that do not belong to the reaction coordinate. Without the coupling to this "bath of modes," there is no way that friction and temperature can be introduced to the problem. Energy flows between the reaction coordinate and this bath. Since the bath is "large" compared to the reaction coordinate, its average kinetic energy sets the temperature of the system and it is also responsible for damping (Caldeira and Leggett, 1983; Garg *et al*, 1985; Onuchic and Wolynes, 1988). For details about this formalism, the reader is referred to the two previous references. However, it is important to note that without the existence of this thermal bath, a rate would not exist. In most simpler treatments, the existence of the bath is included by artificially broadening the energy levels of the reaction coordinate. The strength of the coupling to these "environment modes" determines whether the reaction rate is adiabatic or non-adiabatic. A brief discussion of this topic is presented in Chapter 2 and at the end of this appendix. The interested reader is refered to the three references above.

The tremendous success of Marcus theory leaves us with the question of why such a simple representation based upon a harmonic mode, in most cases overdamped by solvent, is such a good starting point for complex environments? As suggested by eq. 6, electron tunneling occurs only when the donor and acceptor energies are resonant. Therefore, the important nuclear factor that indicates resonance is the energy gap (energy difference) between the donor and acceptor states. In the harmonic case, this energy gap is linearly related to the reaction coordinate. (This relationship appears later in this section, see eq. 9). For this reason, the ideal reaction coordinate for the problem is the energy gap, and the question becomes how complex is its dynamics. This gap may have a very complicated dependence on the conventional nuclear coordinates.

In the case of polar solvents, a single collective reaction coordinate, normally treated as an effective overdamped harmonic mode, has been successful for describing the coupling of the mode's polarization to the electron transfer reaction. The dynamics is described by the overdamped time τ_D/ϵ_0 (τ_D is the Debye time for the solvent and ϵ_0 is its static dielectric constant (Maroncelli *et al*, 1989; Simon, 1988; Barbara and Jerzea, 1990). Recent theoretical advances have shown how a many-dimensional complex solvent can be reduced to this simple representation (Bacgchi, 1989; Onuchic and Wolynes, 1993; Leite and Onuchic, 1995)

Now that we have computed the D-A interaction, we need to compute the ET rate itself. There are numerous approaches to this problem, the most familiar one begins with transition state theory and incorporates corrections as needed. We discuss this strategy at the end of this section (in the context of adiabatic versus non-adiabatic ET rates). The non-adiabatic limit is the ET rate limit of most relevance to biological ET. If the tunneling matrix element is very small (see discussion at the end of the appendix), the ET rate can be written as

$$k_{ET} = \frac{2\pi}{\hbar} T_{DA}^2 \sum_{i,f} P_i^T \delta(E_i - E_f) \tag{8}$$

P_i^T is the thermal distribution of the donor/acceptor state configurations. For the harmonic case described above and assuming Q to be classical,

$$\Delta E = E_i - E_f = M\Omega^2(Q_A - Q_D)Q + \epsilon - \lambda. \tag{9}$$

and $P_i^T(\Delta E)$ can be obtained from the change of variable $Q \rightarrow \Delta E$ since

$$P_i^T(Q) = \frac{1}{\sqrt{2\pi K_B T/M\Omega^2}} \exp - \frac{M\Omega^2(Q - Q_D)^2}{2K_B T}. \tag{10}$$

leading to

$$P_i^T(\Delta E) = \frac{1}{\sqrt{4\pi\lambda K_B T}} \exp - \frac{[\Delta E - (\epsilon - \lambda)]^2}{4\lambda K_B T}. \tag{11}$$

The electron transfer rate becomes

$$k_{ET} = \frac{2\pi}{\hbar} T_{DA}^2 P_i^T(\Delta E = 0) = \frac{2\pi}{\hbar} T_{DA}^2 < \delta(\Delta E) >. \tag{12}$$

This is the well known expression for non-adiabatic ET in the classical limit, i.e.,

$$k_{ET} = \frac{2\pi}{\hbar} T_{DA}^2 \frac{1}{\sqrt{4\pi\lambda K_B T}} \exp\left[-\frac{(\epsilon - \lambda)^2}{4\lambda K_B T}\right]. \tag{13}$$

A full quantum expression can be obtained by replacing

$$< \delta(\Delta E) > \rightarrow < \delta(\Delta \hat{E}) > = \int dt \left\langle T \exp\left[-i \int_0^t d\tau \frac{\Delta \hat{E}(\tau)}{\hbar}\right]\right\rangle. \tag{14}$$

For the case of a single harmonic reaction coordinate, the full quantum expression can be written as (Garg *et al*, 1985; Bialek and Goldstein, 1986)

$$k_{ET} = \frac{T_{DA}^2}{\hbar^2} \int_{-\infty}^{\infty}$$

$$d\tau \exp\left\{ \frac{i\epsilon\tau}{\hbar} - i\frac{\delta Q^2}{\hbar} \int_0^{\infty} \frac{d\omega}{2\pi} \sin(\omega\tau) \frac{\gamma(\omega)}{\omega} \times \frac{\Omega^4}{|\Omega^2 - \omega^2 - i\omega\gamma(\omega)|^2} \right.$$

$$\left. - \frac{\delta Q^2}{\hbar} \int_0^{\infty} \frac{d\omega}{2\pi} [1 - \cos(\omega\tau)] \frac{\gamma(\omega)}{\omega} \times \frac{\Omega^4 \coth(\hbar\omega/2K_B T)}{|\Omega^2 - \omega^2 - i\omega\gamma(\omega)|^2} \right\}, \qquad (15)$$

where $\gamma(\omega)$ is the damping constant. If γ is assumed constant we are in the "ohmic" limit, i.e., the damping force is proportional to the velocity. An approximate solution of eq. 15 may be obtained by applying saddle points or steepest descent methods (Bialek and Goldstein, 1986; Onuchic *et al*, 1990). For underdamped modes there are multiple saddle points, and their contributions must be summed. One obtains

$$k_{ET} = A \exp[-G] \sum_{n=0}^{\infty} \cos(2\pi n\epsilon/\hbar\Omega) \exp[-n\gamma/\Gamma], \qquad (16a)$$

where

$$\Gamma^{-1}(T = 0) = \frac{2\pi\epsilon}{\hbar\Omega^2}, \qquad (16b)$$

$$\Gamma^{-1}(T >> \hbar\Omega/K_B T) \sim \frac{2\pi\epsilon}{\hbar\Omega^2} \times \frac{K_B T}{\hbar\Omega}, \qquad (16c)$$

and

$$A \sim \frac{2\sqrt{\pi} T_{DA}^2}{\hbar} \left\{ 2(\hbar\Omega)^2 S(2\bar{n} + 1) + \ldots \right\}^{-1/2}. \qquad (16d)$$

$$G \sim \frac{(\epsilon - S\hbar\Omega)^2}{2S(\hbar\Omega)^2(2\bar{n} + 1)} - \frac{(\epsilon - S\hbar\Omega)^3}{6S(\hbar\Omega)^3(2\bar{n} + 1)^5} \left[3 + (2n + 1)^2 \right] + \ldots, \qquad (16e)$$

where $\bar{n} = [\exp(\hbar\Omega/K_B T) - 1]^{-1}$ and $\lambda = S\hbar\Omega$. We have expanded G around the term that dominates when $\hbar \to 0$ in order to emphasize that we are looking for quantum corrections to the classical and semiclassical results. For example, if we retain only the $n = 0$ saddle point and only the first term in G, the result reduces to the expression obtained by Hopfield in 1974 (Hopfield, 1974). The so-called quantum limit (Jortner, 1980) is obtained by setting $\gamma \to 0$. In this limit, eq. 18a would reduce to a delta-function that is inhomogeneously broadened.

The discussion to this point has been based on the existence of a single reaction coordinate. Often, in addition to a classical or semiclassical reaction coordinate, quantum modes are also important. These are the inner-sphere modes discussed by Marcus.

The existence of quantum modes complicates the parabolic dependence of the activation barrier on the driving force ϵ. For completeness, we present the rate expression for the case of a transferring electron coupled to two reaction coordinates, a quantum one, y, and a classical one, z. λ_y and λ_z are their respective reorganization energies. y is a high-frequency fully quantum mode, so $\hbar\Omega_y >> K_BT$. Quantum modes coupled to ET are mostly localized vibrations of the ET chromophores (at room temperature, $k_BT = 200\ \mathrm{cm}^{-1}$, covalent chain skeletal vibrations with $\hbar\omega \gg k_BT$ are quantized. In this case (Onuchic, 1987), the electron transfer rate is

$$k_{ET} = \frac{2\pi}{\hbar}\sum_{m_A}\left\{T_{DA}^{eff}(m_A)\right\}^2 \frac{1}{\sqrt{4\pi\lambda_z K_BT}}\exp\left[-\frac{(\epsilon_{m_A}^{eff}-\lambda_z)^2}{4\lambda_z K_BT}\right], \qquad (17a)$$

and

$$T_{DA}^{eff}(m_A) = T_{DA} < n_D = 0|m_A > \quad \text{and} \quad \epsilon_{m_A}^{eff} = \epsilon - m_A\hbar\Omega_y, \qquad (17b)$$

where $|n_D>$ is the n_D'th level for y when the electron is on the donor and $|m_A>$ is the m_A'th level for y when the electron is on the acceptor.

We conclude this section by relating the theoretical approaches presented here with transition state theory, the most common approach for computing chemical reaction rates. We use this strategy to discuss the question of adiabaticity versus non-adiabaticity introduced in Chapter 2. For simplicity, we present a brief discussion for classical barrier crossing. For a full description of the quantum and classical case, the reader is referred to (Onuchic and Wolynes, 1988). The transition state theory of classical barrier crossing replaces the question of how many reactive events occur by the question of how many crossings from reactant to product occur. The problem therefore is much simpler, we only have to calculate the flux across the top of the barrier. (Wigner, 1937; Eyring, 1934). Corrections to this value are normally necessary because multiple crossings can occur for each reactive event. Thus, the transition state rate has to be corrected by a transmission coefficient $\kappa = k/k_{TST}$ that can be estimated by the inverse of the typical number of forward crossings per reactive event.

We now present two examples of κ estimates. First, consider an adiabatic reaction with a diffusive reaction coordinate (Kramer's rate, (Kramers, 1940)). In this case, a typical trajectory resides mostly around the reactant or product well, and a fluctuation rarely causes a barrier crossing. Following the crossing event, once the trajectory has an energy lower than the barrier height by about k_BT, it will typically settle into either

side of the well. The distance from either well to the transition state is l_{TST}. Once the system diffuses this distance it is trapped in one of the two wells. Using a well-known relation for random walks, the number of steps taken in the transition state region is of the order of $(l_{TST}/l)^2$ where l is the corresponding mean free path and is inversely proportional to the damping coefficient, η. η measures the coupling between the reaction coordinate and the bath. In the overdamped limit, the diffusion coefficient is $k_B T/\eta$. The number of recrossings is the fraction of these steps that actually go across the saddle point. Since a step is of length l, this fraction is l/l_{TST}. The transmission coefficient is hence proportional to the mean free path and it is $\kappa = l/l_{TST}$. When the appropriate algebra is performed, we recover exactly the adiabatic limit associated with eq. 2.3 of chapter 2.

The second case we discuss is the question of adiabaticity versus non-adiabaticity. A different but equivalent discussion to the one presented in chapter 2 is the following. Using the idea of recrossings, we can ask the following question: What is the probability of going from reactant (donor) to product (acceptor) in each crossing? This can be answered using the standard Landau-Zener approach to ballistic crossings (Landau, 1932; Zener, 1932), and it can be extended to non-ballistic ones. When these corrections are included, we find exactly the result given by eq. 2.3 in chapter 2 for the overdamped regime. The question of adiabatic versus non-adiabatic rates is a very subtle one. Single crossings may each have a small probability to switch between donor and acceptor states, but if one has multiple crossings per event, these probabilities add up. This interplay between coupling to the environment and Landau-Zener factors is important in determining the nature of the reaction rate.

We hope that with this appendix has provided you with a few new ideas about strategies for computing reaction rates of ET as well as some clues about the origins of standard rate expressions. We have not provided all the details, but this would itself require a separate volume. However, we hope we have provided the key references (and not an overwhelming number of them) that will allow you to deepen your understanding on this subject if you so desire.

Acknowledgments

We are grateful to our collaborators for their thoughtful discussion of these ideas with us. This work is supported by the National Science Foundation (MCB-9316186 and CHE-9257093), the National Institutes of Health (GM48043), and the Department of Energy (DE-FG36-94G010051).

REFERENCES

Barbara PF, Jerzea, W. (1990). TITLE. *Adv. Photochem* 15:1-PAGE.

Bacgchi B. (1989). *Annu. Rev. Phys. Chem.* 40:115-PAGE.

Beratan DN, Hopfield JJ. (1984). TITLE. *J. Chem. Phys.* 81:5753-PAGE.

Bialek W, Bruno WJ, Joseph J, Onuchic JN. (1989). Quantum and Classical Dynamics in Biochemical Reactions. *Photosynthesis Research* 22:15-PAGE.

Bialek W, Goldstein RF. (1986). TITLE. *Phys. Scr.* 34:273-PAGE.

Caldeira AO, Leggett AJ. (1983). TITLE. *Ann. Phys.* 149:374-PAGE.

DeVault D. (1984). *Quantum Mechanical Tunneling in Biological Systems*, Cambridge Press, New York, 2nd ed.

Eyring HJ. (1934). TITLE. *J. Chem. Phys* 3:107-PAGE.

Feher G, Allen J, Okamura M, Rees D. (1989). TITLE. *Nature* 339:111-116.

Garg A, Onuchic JN, Ambegaokar V. (1985). Effect of friction on electron transfer in biomolecules. *J. Chem. Phys.* 83:4491-PAGE.

Hopfield JJ. (1974). TITLE. *Proc. Natl. Acad. Sci (USA)* 71:3640-3644.

Jortner J. (1980). TITLE. *Biochim. Biophys. Acta* 594:139-PAGE.

Kramers HA. (1940). TITLE. *Pysica* 7:284-PAGE.

Landau L. (1932). TITLE. *Sov. Phys.* 1:89-PAGE.

Larsson S. (1981). TITLE. *J. Am. Chem. Soc.* 103:4034-4040.

Leite VBP, Onuchic JN. (1995). Solvent Dynamics in Charge Transfer Reactions. *J. Phys. Chem.* submitted.

Löwdin PO. (1962). TITLE. *J. Math. Phys* 3:969-PAGE.

Marcus RA, Sutin N. (1985). Some Aspects of Electron Transfer in Chemistry and Biology. *Biochim. Biophys. Acta* 811:265-322.

Maroncelli M, McInnis J, Fleming GR. (1989). TITLE. *Science* 243:1674-PAGE.

Miller JR, Beitz JV, Hundleston RK. (1984). *J. Am. Chem. Soc.* 106:5057-PAGE.

Mikkelsen KV, and Ratner MA. (1988). TITLE. *Chem. Rev.* 87:113-153.

Newton MD, Sutin N. (1984). TITLE. *Ann. Rev. Phys. Chem.* 35:437:PAGE.

Onuchic, JN. (1987). Effect of friction on electron transfer – the two reaction coordinate case. *J. Chem. Phys.* 86:3925-3943.

Onuchic JN, Beratan DN, Hopield JJ. (1986). Some aspects of electron transfer reaction dynamics. *J. Phys. Chem.* 90:3707-3721.

Onuchic JN, Beratan DN, Winkler JR, Gray HB. (1992). Pathway Analysis of Protein Electron Transfer Reactions. *Ann. Revs. Biophys. Biomol. Struct.* 21, 349-377.

Onuchic JN, Goldstein RF, Bialek, W. (1990). Biomolecular dynamics – quantum or classical? Results for photosynthetic electron transfer. in: *Perspectives in Photosynthesis, Proceedings of the 22nd Jerusalem Symposium on Quantum Chemistry and Biochemistry*, J. Jortner and B. Pullman, Editors, D. Reidel Publishing Co., Dordrecht, Holland, pp. 211–226.

Onuchic JN, Wolynes, PG. (1988). Classical and quantum pictures of reaction dynamics in condensed matter: resonances, dephasing and all that. *J. Phys. Chem.* 92:6495-PAGE.

Onuchic JN, Wolynes, PG. (1993). Energy Landscapes, Glass Transitions, and Chemical Reaction Dynamics in Biomolecular or Solvent Environment. *J. Chem. Phys.* 98:2218-2224.

Simon JD. (1988). TITLE. *Acc. Chem. Res.* 21:128-PAGE.

Skourtis SS, Beratan DN, Onuchic JN. (1993). A Rigorous Analysis of the Two-State Reduction for Electron and Hole Transfer in Bridge-Mediated Electron-Transfer Reactions. *Chem. Phys.* 176:501-PAGE.

Skourtis SS, Onuchic JN. (1993). Effective Two-State Systems in Bridge-Mediated Electron Transfer: A Green's Function Analysis for One-Electron Hamiltonians. *Chem. Phys. Let.* 209:171-177.

Ulstrup J. (1979). *Charge Transfer Process in Condensed Matter*, Springer Verlag, New York.

Wigner EJ. (1937). *J. Chem. Phys.* 5:720-PAGE.

Wolynes, PG. (1987). TITLE. *J. Chem. Phys.* 86:1957-PAGE.

Zener C. (1932). TITLE. *Proc. R. Soc. London, A* 137:696-PAGE.